Rising Temperatures, Rising Risks: Changes in Chinese Children's Heat Exposure between1990 and 2020

Kai Feng, Marco M. Laghi, Jere R. Behrman, Emily Hannum, and Fan Wang*

April 15, 2024

Please click here for latest version of the paper.

Abstract

The frequency and intensity of heat waves are increasing as the earth's climate warms, but how these trends translate to changes in children's heat exposure is not well established. Using the case of China, home to approximately 250 million children in 2020, we developed a *double-dual-distributional (DDD) framework* to analyze duration and intensity of heat exposure among children. We found substantial, heterogeneous increases in the share of children at risk and time exposed to high heat. From 1990 to 2020, there was an increase of 238 hours in children's average annual exposure to moderate or stronger heat. The share of children subjected to over 18 weeks of such heat stress more than doubled, increasing from 6.7% to 13.7%. Approximately half of the overall change in child high-heat exposure was driven by heat increases, with the rest driven by shifts in the child population across regions. This result underscores a point relevant beyond China: shifts in the location of the child population, alongside temperature changes, are important drivers of children's changing heat exposure risk over time. Our framework is novel in estimating the share of children at risk of extreme temperature exposures across different temperature thresholds and shares of time exposed to heat, jointly considering the geographical and temporal distributions of heat and children, and allowing for estimates at more and less extreme thresholds.

Keywords: Extreme heat, children, China, geographic distribution of children

*Kai Feng: Department of Sociology and Population Studies Center, University of Pennsylvania, Philadelphia, Pennsylvania, USA; Marco M. Laghi: Department of Sociology, New York University, New York, NY, USA; Center for Applied Social and Economic Research, NYU Shanghai, Shanghai, China; Jere R. Behrman: Departments of Economics and Sociology and Population Studies Center, University of Pennsylvania, Philadelphia, Pennsylvania, USA; Emily Hannum: Department of Sociology and Population Studies Center, University of Pennsylvania, Philadelphia, Pennsylvania, USA; Fan Wang: Department of Economics, University of Houston, Houston, Texas, USA. This paper is supported by National Science Foundation Grants 1756738 and 2230615.

1 Introduction

Extreme heat exposure represents a significant and growing threat to human health and welfare (Carleton and Hsiang 2016; Ebi et al. 2021; Gasparrini et al. 2015; Kovats and Hajat 2008; Mora et al. 2017), with research increasingly highlighting its disproportionate impact on vulnerable populations (Harrington et al. 2016; Hsu et al. 2021; Li et al. 2016; Mitchell and Chakraborty 2015). Among population subgroups, children are particularly susceptible to the detrimental effects of heat exposure (Connon and Dominelli 2022a, 2022b; Park, Behrer, and Goodman 2021; Prentice et al. 2024; Zivin and Shrader 2016). Studies have shown that extreme heat directly impacts children by undermining their nutrition (Baker and Anttila-Hughes 2020), impairing cognitive and skill development (Park, Behrer, and Goodman 2021), and escalating the rates of heat-related illnesses and mortality (Helldén et al. 2021; Zivin and Shrader 2016). Moreover, the negative effects of heat exposure can begin as early as the prenatal stage (Edwards, Saunders, and Shiota 2003). Research has linked high temperatures to increased instances of preterm births and babies born with low birth weights (Grace et al. 2015; Liu et al. 2022; Ren et al. 2023). Additionally, extreme heat indirectly affects children by exacerbating droughts and associated food insecurity (Chavez et al. 2015; Cooper et al. 2019; Sun et al. 2024), intensifying tropical disasters (Grinsted, Moore, and Jevrejeva 2013; Van Aalst 2006), facilitating the spread of infectious diseases (Onozuka and Hashizume 2011; Xu, Liu, et al. 2014), and heightening the risk of violent conflicts (Akresh 2016; Hsiang, Burke, and Miguel 2013); to all of which children are increasingly or particularly sensitive.

Climatic change has both prolonged and intensified extreme heat (Jones et al. 2015; Li and Zha 2020; Sun et al. 2022; Sun et al. 2014; Tuholske et al. 2021). Projections suggest a significant rise in the burden of heat exposure on populations, a trend attributed to both climatic changes and the increased populations exposed to these changes (Jones et al. 2018; Liu et al. 2017). Yet, few studies except those by UNICEF (2021, 2022) focus on change in exposure among the child population despite the vulnerability of children and youth to heat exposure. In addition, the prevalent approach in these studies is to measure the total burden as person-time, calculated as the total population multiplied by the total time spent above a specific temperature threshold (Jones et al. 2015; Liu et al. 2017; Sun et al. 2022; Tuholske et al. 2021), while overlooking the shifting concentration of populations that might experience these temperature changes, the varying distribution of burden across different risk levels and the diverse durations of exposure to these risks.

Using the case of China, home to approximately 250 million children ages 0-14 in the year 2020 (National Bureau of Statistics of China 2021), this study estimated children's changing exposure to extreme heat by linking county-level child population data to the hourly Universal Thermal Climate Index (UTCI), a bioclimatic index for assessing the physiological comfort of the human body (Bröde et al. 2012; Jendritzky, Dear, and Havenith 2012; Jendritzky and Höppe 2017), across two censuses spanning 30 years (1990-2020). We proposed a convenient, low-data-demand framework for estimating the share of children at risk of extreme heat exposures. This framework, referred to as *double-dual-distributional (DDD) framework*, jointly considered heat thresholds and the share of time exposed to such heat thresholds. Additionally, it allowed for computing population-group-specific heat exposure changes over time that account for changes in both the geographical and temporal distributions of heat and children.

We found substantial increases in the average high-heat exposure for children and the share of children at risk. Specifically, the average child was exposed to moderate or higher levels of heat stress for an additional 238 hours in 2020 in comparison to 1990. The share of children subjected to over 18 weeks of such heat stress more than doubled, increasing from 6.7% to 13.7%. We also found that approximately half of the overall change in child high-heat exposure between 1990 and 2020 is driven by heat increases and the rest was driven by cross-regional shifts in the child population towards locations that had higher heat, illustrating the importance of *both* child population distributions and heat patterns. Finally, we highlighted significant regional disparities: In Eastern China, its most developed region, there was a marked increase in the duration of children's heat exposure from 1990 to 2020, even though the exposure levels were already high in 1990. Conversely, the Central region, which had comparable exposure levels as the Eastern in 1990, experienced only a minimal increase in exposure from 1990 to 2020.

2 Methods and Data

Methods. In this section, we summarize our double-dual-distributional (DDD) framework for measuring child population at risk of heat exposure. Within a particular span of time in a region, our DDD framework develops two statistics for temperature exposure risks building on two types of distributions and two types of thresholds. The two distributions are the distribution of location-specific temperature and the distribution of population across locations conditional on population group (children). The two thresholds are temperature thresholds (intensity of exposure) for extreme-temperature exposure and time thresholds (duration of exposure) for share of time exposed to extreme-temperature. The first risk statistic captures the risk of extreme temperature exposure facing the average child, measured in units of share of time the average child is exposed to extreme temperatures. The second risk statistic captures the distribution of risk among children, measured in units of the share of child population exposed to extreme temperatures for different durations of time.

In studies that consider population heat exposures, a prevalent metric for assessing heat exposure is the change in exposure in total person-time. The person-days of heat exposure in a place at time t can be computed, for example, by multiplying the days during which the maximum temperature exceeds a threshold level with the total population residing in a place at time t. Aggregate person-time statistics have two limitations. First, when comparing exposures over time, aggregate person-time statistics will capture changes in aggregate population size over time in addition to changes in average heat exposure burdens. For example, if the rate of population decline surpasses the rate of temperature increase, the resultant person-time estimates may diminish over time. Second, the person-time aggregate provides a single statistic of exposure for a region or country, overlooking the heterogeneities in ambient exposure changes across populations residing in locations with differing climatic change experiences. In addition to considering both climatic and population distributions, as done in person-time statistics, our DDD framework captures heterogeneities across time and space by measuring changes in the percentages of children experiencing different intensities of heat stress (temperature thresholds) for different durations over time (time thresholds).

In the closest related work, UNICEF (2022) estimates the aggregate number of children at risk of heat exposure based on the aggregate population share of children. The most closely-related studies focusing on all population groups generally provide different types of average aggregated statistics. Our framework is the first to jointly apply the double-distributions to compute the share of children (and population generally) at risk of the double-thresholds of exposure. We provide a detailed description of our methods in the appendix.

We implemented our framework in the setting of China between 1990 and 2020. In this empirical application, we considered each span of time as one year, we approximated continuous ambient temperature exposures based on hourly estimates of temperature, and we approximated fine-grained measures of locations where the temperature gradient is non-zero with counties (3rd level administrative units) in China. For the temperature thresholds, we considered a range of thresholds but focused our analysis on key thresholds for extreme-heat commonly used in the literature. For time thresholds, we considered different shares of time during the course of the year exposed to temperatures above the thresholds considered. Our method is also straight-forward to implement in other settings where tabular population data at relatively fine-grained level and location-specific climate data are available.

Data. To measure heat, we used the fifth generation of the European Centre for Medium-Range Weather Forecasts (ECMWF) atmospheric reanalyses of the global climate: the ERA5-HEAT dataset (Napoli 2020). ERA5-HEAT, a distinct advancement from its predecessors, offers hourly data on numerous climatic variables with a spatial resolution of 0.25 degrees, including the Universal Thermal Climate Index (UTCI). The UTCI provides an integrative measure of the human-perceived equivalent temperature, taking into account factors like air temperature, humidity, wind speed, and radiant heat (Bröde et al. 2012; Jendritzky, Dear, and Havenith 2012; Jendritzky and Höppe 2017). UTCI is widely used and provides a single value representing the perceived thermal stress on the human body. When UTCI is between 26°C and 32°C, it indicates moderate heat stress on the human body, signifying warm conditions where individuals may start to feel uncomfortable, especially if engaging in physical activity. As the UTCI value increases, the level of thermal stress on the human body intensifies. UTCI between 32°C and 38°C indicate strong heat stress, whereas UTCI between 38°C and 46°C indicate very strong heat stress. We utilized the UTCI in this paper.

For population data, we utilized Chinese census data for the years 1990 and 2020 (All China Market Research Ltd 2022; Beijing Hua tong ren shi chang xin xi you xian ze ren gong si 2005a, 2005b; China Data Lab 2020). County-level population data, shapefiles, and microdata on demographic characteristics of age and gender were extracted and used to construct the population exposures by county. For regional analysis, temperature and population data were sorted by province and assigned to one of the four recognized economic regions of China (National Bureau of Statistics of China 2011).

3 Results

Increase in the Average Share of Time Exposed to Heat for Children The three-colored backgrounds in Figure 1 reflect the stress categories associated with different UTCI thresholds. This figure depicts the *percentage point change*s (Panel a) and *percentage changes* (Panel b) in the average share of time in heat stress for children from 1990 to 2020 using three different time periods: all annual hours, daytime hours (6 a.m. - 10 p.m.), and April to September hours as the hot months of the year. Across the three time-frame specifications, children's share of time in heat stress increased in China from 1990 to 2020 across all UTCI heat thresholds. The largest percentage point change (Figure 1 Panel a) occurred when considering only hours in hot months, followed by daytime hours, and then all annual hours. The percentage changes (Figure 1 Panel b) largely overlaped across the three time-frame specifications.

When all hours were considered, an average child in China experienced 20.09% of her total hours in 1990 at 26°C UTCI or above this threshold. By 2020, this percentage increased to 22.8%, representing a 2.7 percentage point (Figure 1 Panel a) and 13.5% increase in annual average exposure duration (Figure 1 Panel b), which corresponded to an increase over 30 years of 238 hours of additional moderate or stronger heat-stress exposure.

Across all heat thresholds, children's average share of time at risk of heat stress increased. While the percentage points increases were smaller at higher heat thresholds, the percentage increases in the average child share of time exposed to UTCI thresholds between 26°C to 40°C were similar and ranged between 14% and 18%. For example, the average duration of children's exposure to UTCI at or above 32°C increased by 1.1 percentage points, reflecting a 14.7% rise as compared to the levels observed in 1990. These results also indicated that approximately 40% (calculated as $1 - \frac{2.7-1.1}{2.7} \approx 0.4$) of the increase in average heat exposure at the 26°C threshold can be attributed to the escalation in exposure to strong or above heat stress exceeding the 32°C threshold. Tables D.1 and D.2 in the Appendix document the children's average share of time at risk of heat stress in 1990 and 2020 by UTCI thresholds using the three different time periods defined above and used in Figure 1.

Increases in Share of Children at Risk of Heat Exposure. While the previous results focus on heat exposure for the average child in China, they do not provide information on how many children were increasingly at risk of heat exposure. In this section, given the changing distribution of heat and children across counties in China, we examined whether the *percentage* of children most affected by heat stress has also changed over time.

We computed the share of children at risk by jointly considering two thresholds of risks: a threshold for the level of heat stress exposure (intensity) and a threshold for the share of annual hours (duration) exposed to heat stress above a particular threshold. Figure 2 illustrates the combination of selected thresholds for the duration of time exposed to heat stress (from 4% to 36%) and the intensity of heat stress (from above 26°C to above 38°C). Appendix tables D.3 and D.4 provide tabulations at additional thresholds.

Exposure to at least some moderate heat stress was nearly universal among children in China. In 1990 (Figure 2 Panel a) and 2020 (Figure 2 Panel b), respectively, 97.2% and 97.7% of children experienced at least 4% of their hours, or over 2 weeks, in moderate or stronger heat stress (i.e. UTCI $\geqslant$ 26°C). As the duration of exposure to heat stress increased, the share of affected children decreased.

The share of children enduring prolonged exposure to heat stress increased substantially from 1990 to 2020. In 1990, 6.7% of children experienced moderate or stronger heat stress for more than 36% of their total hours, or equivalently, for over 16 weeks. By 2020, this number rose to 13.7%, marking an increase of 7.0 percentage points (Figure 2 Panel c) or 106% (Table D.4 Panel b). In other words, the share of children experiencing *at least* moderate heat stress for *at least* 32% of their total hours in 2020 more than doubled compared to 1990.

A substantial increase in the share of children experiencing heat stress can be observed across various combinations of heat stress intensity and duration. For example, 11.2% (Figure 2 Panel a) of children had at least 12% of their total hours, or 6 weeks at strong heat stress or above ($\geqslant$32°C). This number rose to 18.6% in 2020 (Figure 2 Panel b), representing a 7.4 percentage point (Figure 2 Panel c) or 66.3% increase (Table D.4 Panel b).

Especially alarming were rapid increases in the share of children at risk for very strong heat stress shown in Figure 2. In particular, the share of children experiencing at least 4% of their total hours for at least very strong heat stress increased from 0.1% to 1.8%. While the share of children exposed to these extreme risk levels remained small, these increases represented approximately an 18-fold jump in the share of children at these high exposure risk levels. With 249.9 million children between ages 0 to 15 in China in 2020, 1.8% amounts to 1.5 million children.

Decomposing the Contributions of Changes in Climate and Population. Figure 3 depicts results from a decomposition analysis at the national level. This analysis illustrates the extent to which changes in children's heat exposure over time can be attributed to shifts in the distribution of the child population, or due to changes in UTCI driven by meteorological changes. In this decomposition exercise, we altered one distribution (either children's population or UTCI) to 2020 levels while keeping the other constant at 1990 levels, without modeling mechanisms of change. In Appendix Table D.5, we also present decomposition results in China's Eastern and Northeastern regions.

Figure 3 demonstrates that the increase in an average child's heat stress exposure from 1990 to 2020 resulted from both climate change and shifts in children's population distribution. For at least strong ($\geqslant 32\,^{\circ}$C) and at least moderate heat ($\geqslant 26\,^{\circ}$C) stress levels, child population distribution shifts accounted for 48% and 50% of the actual change, respectively. UTCI distribution shifts accounted for 42% and 40% of the actual changes, respectively. Unexplained residual changes were due to interactions between shifts in climatic and population distributions.

While both population distribution change and climate change contributed to the rise in the average child's heat stress exposure, regional decomposition analysis showed varying impacts within regions (see Appendix Table D.5). Specifically, changes in population distribution accounted for about 1/3 of the exposure shifts in the Eastern region and less than 1/5 in the Northeastern region. This suggests that cross-regional shifts in children's distribution, such as migration to the Eastern region or fertility decline in the Northeastern region, played more-significant roles in explaining the population results observed nationally.

Figure 3 also indicates that at higher UTCI thresholds, the influence of changes in population distribution diminished. Nationally, the contribution of population distribution to heat stress exposure declined with increasing heat thresholds, from 50% at UTCI above 26 °C to 39% at UTCI 36 °C. Similarly, the contribution of population distribution declined from 38% to 19% in the Eastern region and from 16% to 5% in the Northeastern region over the same sets of UTCI threshold increments. This suggests that the rise in more extreme heat exposures was primarily a result of climatic change, rather than population shifts to already hotter areas.

Changes in Children's Heat Exposure Across Regions. Shifting to cross-region analysis, we show in Figure 4 Panels (a) and (b) the average share of annual time at risk of heat stress for children in 1990 and 2020 across four economic regions of China. Figure 4 (c) shows the percentage point (pp) change between 1990 and 2020 across these regions.

Children in both the Central and Eastern regions experienced high levels of heat stress exposure. For instance, in 1990, an average child in the Eastern and Central regions faced at least moderate heat stress (above UTCI 26 °C) 23.6% and 23.4% of the time, and at least strong heat stress (above UTCI 26 °C) 8.4% and 9.3% of the time, respectively. The share of time exposed to at least moderate or at least strong heat stress in these two regions remained high in 2020 as shown in Figure 4 (b). The percentage point changes in the share of time at risk of heat exposure were notable across various UTCI thresholds in the Eastern region, with a 4.4 pp at above 26 °C and a 1.7 percentage point increase at 32 °C. In contrast, for the central region, the changes in the share of time remained below 1 pp across UTCI thresholds (Figure 4 (c)). The comparison indicates that although children in both regions spent a significant amount of time exposed to heat, those in the Eastern region faced a heightened challenge in adapting to heat stress owing to the rapid increase in exposure duration.

Compared to the Eastern and Central regions, the Northeastern region had relatively low average child heat exposure in 1990. However, the average child's share of annual time in the Northeastern region increased 19% ($\geqslant$ 26 °C) and 36% ($\geqslant$ 29 °C) for at least moderate heat stress and 106% ($\geqslant$ 32 °C) and 457% ($\geqslant$ 35 °C) for at least strong heat stress. In 2020, the average Northeastern-region child experienced 8.9% and 2.4% of her time under at least moderate ($\geqslant$ 26 °C) and at least strong ($\geqslant$ 32 °C) heat stress. While child heat stress in the Northeastern region remained much lower than that in the Central and Eastern regions, but the rapid increases indicates potential challenges for a population that is not accustomed to heat to protect children from emerging occurances of heat stress.

Table D.7 and D.8 in Appendix provide additional results on changes in children's shares of annual time exposed to heat stress at the province level. In 2020, Hainan (Eastern), Guangdong (Eastern), Guangxi (Western), Jiangxi (Central), and Fujian (Eastern) were generally ranked as the top 1 to 5 provinces respectively in terms of the average share of child time exposed to heat across all UTCI thresholds. Specifically, in 2020, children in Hainan, Guangdong, Guangxi, Jiangxi, and Fujian had on average 19.2%, 15.2%, 13.2%, 12.8%, and 11.8% share of time exposed to at least strong heat stress (UTCI $\geqslant$ 32 °C), which represented respective increases of 17%, 20%, 8%, 16%, and 54% in share of time exposed compared to 1990.

While the Northeastern and Eastern regions' provinces (excluding Jiangsu) experienced substantial increases in heat exposure, provinces in the Central and Western regions experienced limited exposure increases and reductions. In particular, provinces of Hubei and Anhui in Central China and Gansu, Guizhou, and Qinghai in Western China generally experienced reductions in average child heat exposures across UTCI thresholds. Additionally, children in Qinghai and Xizang (Tibet) in the Western region continued to have generally no exposure to at least moderate heat stress.

4 Discussion

As climate change intensifies, the exposure of children to extreme heat is a critical concern in human development and public health (Connon and Dominelli 2022a; Park, Behrer, and Goodman 2021; Prentice et al. 2024; Zivin and Shrader 2016), but it has received limited attention in research. This study presents a analysis of children's exposure to extreme heat in China over the past 30 years. Leveraging on both geographical and temporal distributions of heat and children, our study uncovers a significant increase in children's exposure to moderate or stronger heat by an average of 238 hours from 1990 to 2020. The share of children experiencing over 18 weeks of such heat stress more than doubled, indicating growing vulnerability among this group.

Our results highlight a compounded effect of rising temperatures and shifts in child population geographical distribution, particularly in a populous nation like China. The exposure to higher heat stress levels, especially in the Eastern region, underscored the urgency for targeted interventions. This includes enhancing climate resilience and heat-stress mitigation strategies, especially in urban areas where the heat-island effect may exacerbate exposure (Masson et al. 2020). Additionally, our findings underscored the importance of considering demographic changes alongside climate trends, as population shifts contributed significantly to the observed increase in heat exposure (Jones et al. 2015; Liu et al. 2017).

Conceptually, our approach to analyzing population-climatic exposure changes moved from the conventional metric of total person-time for measuring overall heat exposure burden to a *double-dual-distributional framework* that considered both exposure intensity and exposure duration. This approach enabled a comprehensive analysis of the share of children experiencing 1) varying degrees of heat stress (exposure intensity) over 2) varying spans of time (exposure duration). It allowed for cross-time and cross-location comparisons. Moreover, this approach emphasized shifts in population spatial distribution rather than changes in total population numbers, making it particularly valuable in identifying populations at risk of exposure in scenarios of depopulation.

Our framework combined tabular population census data with gridded climate data across time and space. We provided a model for integrating population and climate data for climate and social scientists interested in examining the changing exposures of different populations to climate and environmental hazards. While the availability of subnational and consistent global population data across long time spans is limited, subnational census data are publicly available for many countries across time and could be merged with publicly available global temperature and other climate data to explore changes in population-based climatic exposures over time.

Our study has several limitations. Firstly, we examined ambient exposures, and did not explore how the same ambient heat stress might impact heterogeneously individuals residing in the same location but coming from varied socio-economic backgrounds. Socioeconomic disparities in access to air conditioning or other adaptive resources can significantly influence the actual experience of heat stress (Xu, Sheffield, et al. 2014; Zivin and Shrader 2016). At an aggregate level, regions with similar ambient exposures but at different stages of economic development could also have varied levels of adaptabilities to the same heat stress. Furthermore, our analysis defined heat stress based on duration of exposure over the course of one year, without considerations of potential mobility and movement of child populations. Future research may benefit from examining the heterogeneities in exposure by exploiting the migratory paths of children and households using panel data or retrospective surveys (Mueller, Gray, and Kosec 2014). Finally, the use of county-level data, while detailed, might still miss finer nuances of heat stress, especially in densely populated urban areas where microclimatic variations were significant (Zhou et al. 2015). Future research can build upon our study by integrating our frameworks with various definitions of heat exposure and using more fine-grained geographic units.

References

Akresh, Richard. 2016. "Climate Change, Conflict, and Children." *The Future of Children* 26 (1): 51–71. https://www.jstor.org/stable/43755230.

All China Market Research Ltd. 2022. *2020 China County Population Census Data with GIS Maps.*

Baker, Rachel E., and Jesse Anttila-Hughes. 2020. "Characterizing the Contribution of High Temperatures to Child Undernourishment in Sub-Saharan Africa." *Scientific Reports* 10, no. 1 (November 2, 2020): 18796. https://doi.org/10.1038/s41598-020-74942-9.

Beijing Hua tong ren shi chang xin xi you xian ze ren gong si. 2005a. *1990 County Boundaries of China with Population Census Data, Part 1 & 2. [Shapefile].* https://geo.nyu.edu/catalog/nyu-2451-34775.

———. 2005b. *China Historical 2000 County Population Census Data.* https://geo.nyu.edu/catalog/harvard-ch-census2000.

Bröde, Peter, Dusan Fiala, Krzysztof Błażejczyk, Ingvar Holmér, Gerd Jendritzky, Bernhard Kampmann, Birger Tinz, et al. 2012. "Deriving the Operational Procedure for the Universal Thermal Climate Index (UTCI)." *International Journal of Biometeorology* 56, no. 3 (May 1, 2012): 481–494. https://doi.org/10.1007/s00484-011-0454-1.

Carleton, Tamma A., and Solomon M. Hsiang. 2016. "Social and Economic Impacts of Climate." *Science* 353, no. 6304 (September 9, 2016): aad9837. https://doi.org/10.1126/science.aad9837.

Chavez, Erik, Gordon Conway, Michael Ghil, and Marc Sadler. 2015. "An End-to-End Assessment of Extreme Weather Impacts on Food Security." *Nature Climate Change* 5, no. 11 (November): 997–1001. https://doi.org/10.1038/nclimate2747.

China Data Lab. 2020. *China County Map with 2000-201o Population Census Data.* In collaboration with China Data Lab. https://doi.org/10.7910/DVN/VKGEBX.

Connon, Irena, and Lena Dominelli. 2022a. *Rapid Literature Review: Children and Heat Waves.* UNICEF Children's Climate Change Risk Index (CCRI). Data for Children Collaborative, September. https://www.dataforchildrencollaborative.com/outputs/rapidreview-heatwaves-tmha3.

———. 2022b. *Systematic Review of the Literature: Findings, Outcomes and Policy Recommendations.* UNICEF Children's Climate Change Risk Index (CCRI). Data for Children Collabortive and UNICEF, April. http://dspace.stir.ac.uk/handle/1893/34193.

Cooper, Matthew W., Molly E. Brown, Stefan Hochrainer-Stigler, Georg Pflug, Ian McCallum, Steffen Fritz, Julie Silva, et al. 2019. "Mapping the Effects of Drought on Child Stunting." *Proceedings of the National Academy of Sciences* 116, no. 35 (August 27, 2019): 17219–17224. https://doi.org/10.1073/pnas.1905228116.

Ebi, Kristie L, Anthony Capon, Peter Berry, Carolyn Broderick, Richard De Dear, George Havenith, Yasushi Honda, et al. 2021. "Hot Weather and Heat Extremes: Health Risks." *The Lancet* 398, no. 10301 (August): 698–708. https://doi.org/10.1016/S0140-6736(21)01208-3.

Edwards, M. J., R. D. Saunders, and K. Shiota. 2003. "Effects of Heat on Embryos and Foetuses." *International Journal of Hyperthermia* 19, no. 3 (January 1, 2003): 295–324. https://doi.org/10.1080/0265673021000039628.

Gasparrini, Antonio, Yuming Guo, Masahiro Hashizume, Eric Lavigne, Antonella Zanobetti, Joel Schwartz, Aurelio Tobias, et al. 2015. "Mortality Risk Attributable to High and Low Ambient Temperature: A Multicountry Observational Study." *The Lancet* 386, no. 9991 (July 25, 2015): 369–375. https://doi.org/10.1016/S0140-6736(14)62114-0.

Grace, Kathryn, Frank Davenport, Heidi Hanson, Christopher Funk, and Shraddhanand Shukla. 2015. "Linking Climate Change and Health Outcomes: Examining the Relationship Between Temperature, Precipitation and Birth Weight in Africa." *Global Environmental Change* 35 (November 1, 2015): 125–137. https://doi.org/10.1016/j.gloenvcha.2015.06.010.

Grinsted, Aslak, John C. Moore, and Svetlana Jevrejeva. 2013. "Projected Atlantic Hurricane Surge Threat from Rising Temperatures." *Proceedings of the National Academy of Sciences* 110, no. 14 (April 2, 2013): 5369–5373. https://doi.org/10.1073/pnas.1209980110.

Harrington, Luke J., David J. Frame, Erich M. Fischer, Ed Hawkins, Manoj Joshi, and Chris D. Jones. 2016. "Poorest Countries Experience Earlier Anthropogenic Emergence of Daily Temperature Extremes." *Environmental Research Letters* 11, no. 5 (May): 055007. https://doi.org/10.1088/1748-9326/11/5/055007.

Helldén, Daniel, Camilla Andersson, Maria Nilsson, Kristie L. Ebi, Peter Friberg, and Tobias Alfvén. 2021. "Climate Change and Child Health: A Scoping Review and an Expanded Conceptual Framework." *The Lancet Planetary Health* 5, no. 3 (March 1, 2021): e164–e175. https://doi.org/10.1016/S2542-5196(20)30274-6.

Hsiang, Solomon M., Marshall Burke, and Edward Miguel. 2013. "Quantifying the Influence of Climate on Human Conflict." *Science* 341, no. 6151 (September 13, 2013): 1235367. https://doi.org/10.1126/science.1235367.

Hsu, Angel, Glenn Sheriff, Tirthankar Chakraborty, and Diego Manya. 2021. "Disproportionate Exposure to Urban Heat Island Intensity Across Major US Cities." *Nature Communications* 12, no. 1 (May 25, 2021): 2721. https://doi.org/10.1038/s41467-021-22799-5.

Jendritzky, Gerd, Richard de Dear, and George Havenith. 2012. "UTCI—Why Another Thermal Index?" *International Journal of Biometeorology* 56, no. 3 (May 1, 2012): 421–428. https://doi.org/10.1007/s00484-011-0513-7.

Jendritzky, Gerd, and Peter Höppe. 2017. "The UTCI and the ISB." *International Journal of Biometeorology* 61, no. 1 (September 1, 2017): 23–27. https://doi.org/10.1007/s00484-017-1390-5.

Jones, Bryan, Brian C. O'Neill, Larry McDaniel, Seth McGinnis, Linda O. Mearns, and Claudia Tebaldi. 2015. "Future Population Exposure to US Heat Extremes." *Nature Climate Change* 5, no. 7 (July): 652–655. https://doi.org/10.1038/nclimate2631.

Jones, Bryan, Claudia Tebaldi, Brian C. O'Neill, Keith Oleson, and Jing Gao. 2018. "Avoiding Population Exposure to Heat-Related Extremes: Demographic Change Vs Climate Change." *Climatic Change* 146, no. 3 (February 1, 2018): 423–437. https://doi.org/10.1007/s10584-017-2133-7.

Kovats, R. Sari, and Shakoor Hajat. 2008. "Heat Stress and Public Health: A Critical Review." *Annual Review of Public Health* 29 (Volume 29, 2008 2008): 41–55. https://doi.org/10.1146/annurev.publhealth.29.020907.090843.

Li, Long, and Yong Zha. 2020. "Population Exposure to Extreme Heat in China: Frequency, Intensity, Duration and Temporal Trends." *Sustainable Cities and Society* 60 (September): 102282. https://doi.org/10.1016/j.scs.2020.102282.

Li, Tiantian, Radley M. Horton, Daniel A. Bader, Maigeng Zhou, Xudong Liang, Jie Ban, Qinghua Sun, et al. 2016. "Aging Will Amplify the Heat-Related Mortality Risk Under a Changing Climate: Projection for the Elderly in Beijing, China." *Scientific Reports* 6, no. 1 (June 20, 2016): 28161. https://doi.org/10.1038/srep28161.

Liu, Xiaoying, Jere Behrman, Emily Hannum, Fan Wang, and Qingguo Zhao. 2022. "Same Environment, Stratified Impacts? Air Pollution, Extreme Temperatures, and Birth Weight in South China." *Social Science Research* 105 (July 1, 2022): 102691. https://doi.org/10.1016/j.ssresearch.2021.102691.

Liu, Zhao, Bruce Anderson, Kai Yan, Weihua Dong, Hua Liao, and Peijun Shi. 2017. "Global and Regional Changes in Exposure to Extreme Heat and the Relative Contributions of

Climate and Population Change." *Scientific Reports* 7, no. 1 (March 7, 2017): 43909. https://doi.org/10.1038/srep43909.

Masson, Valéry, Aude Lemonsu, Julia Hidalgo, and James Voogt. 2020. "Urban Climates and Climate Change." *Annual Review of Environment and Resources* 45 (Volume 45, 2020 2020): 411–444. https://doi.org/10.1146/annurev-environ-012320-083623.

Mitchell, Bruce C., and Jayajit Chakraborty. 2015. "Landscapes of Thermal Inequity: Disproportionate Exposure to Urban Heat in the Three Largest US Cities." *Environmental Research Letters* 10, no. 11 (November): 115005. https://doi.org/10.1088/1748-9326/10/11/115005.

Mora, Camilo, Bénédicte Dousset, Iain R. Caldwell, Farrah E. Powell, Rollan C. Geronimo, Coral R. Bielecki, Chelsie W. W. Counsell, et al. 2017. "Global Risk of Deadly Heat." *Nature Climate Change* 7, no. 7 (July): 501–506. https://doi.org/10.1038/nclimate3322.

Mueller, V., C. Gray, and K. Kosec. 2014. "Heat Stress Increases Long-Term Human Migration in Rural Pakistan." *Nature Climate Change* 4, no. 3 (March): 182–185. https://doi.org/10.1038/nclimate2103.

Napoli, Claudia Di. 2020. *Thermal Comfort Indices Derived from ERA5 Reanalysis.* https://doi.org/10.24381/CDS.553B7518.

National Bureau of Statistics of China. 2011. *[Method of Dividing the East, West, Central and Northeast Regions].* Beijing: State Council of China, June 13, 2011. https://web.archive.org/web/20190323041213/http://www.stats.gov.cn/ztjc/zthd/sjtjr/dejtjkfr/tjkp/201106/t20110613_71947.htm.

———. 2021. *Main Data of the Seventh National Population Census.* Beijing: State Council of China, May 11, 2021. https://www.unicef.cn/en/media/24511/file/What%20the%202020%20Census%20Can%20Tell%20Us%20About%20Children%20in%20China%20Facts%20and%20Figures.pdf.

Onozuka, Daisuke, and Masahiro Hashizume. 2011. "The Influence of Temperature and Humidity on the Incidence of Hand, Foot, and Mouth Disease in Japan." *Science of The Total Environment* 410-411 (December 1, 2011): 119–125. https://doi.org/10.1016/j.scitotenv.2011.09.055.

Park, R. Jisung, A. Patrick Behrer, and Joshua Goodman. 2021. "Learning is Inhibited by Heat Exposure, Both Internationally and Within the United States." *Nature Human Behaviour* 5, no. 1 (January): 19–27. https://doi.org/10.1038/s41562-020-00959-9.

Pebesma, Edzer. 2018. "Simple Features for R: Standardized Support for Spatial Vector Data." *The R Journal* 10 (1): 439–446. https://doi.org/10.32614/RJ-2018-009.

Prentice, Caitlin M., Francis Vergunst, Kelton Minor, and Helen L. Berry. 2024. "Education Outcomes in the Era of Global Climate Change." *Nature Climate Change* 14, no. 3 (March): 214–224. https://doi.org/10.1038/s41558-024-01945-z.

Ren, Meng, Chunying Zhang, Jiangli Di, Huiqi Chen, Aiqun Huang, John S. Ji, Wannian Liang, et al. 2023. "Exploration of the Preterm Birth Risk-Related Heat Event Thresholds for Pregnant Women: A Population-Based Cohort Study in China." *The Lancet Regional Health - Western Pacific* 37 (August): 100785. https://doi.org/10.1016/j.lanwpc.2023.100785.

Sun, Xuerong, Fei Ge, Yi Fan, Shoupeng Zhu, and Quanliang Chen. 2022. "Will Population Exposure to Heat Extremes Intensify Over Southeast Asia in a Warmer World?" *Environmental Research Letters* 17, no. 4 (March): 044006. https://doi.org/10.1088/1748-9326/ac48b6.

Sun, Yida, Shupeng Zhu, Daoping Wang, Jianping Duan, Hui Lu, Hao Yin, Chang Tan, et al. 2024. "Global Supply Chains Amplify Economic Costs of Future Extreme Heat Risk." *Nature* 627, no. 8005 (March 28, 2024): 797–804. https://doi.org/10.1038/s41586-024-07147-z.

Sun, Ying, Xuebin Zhang, Francis W. Zwiers, Lianchun Song, Hui Wan, Ting Hu, Hong Yin, et al. 2014. "Rapid Increase in the Risk of Extreme Summer Heat in Eastern China." *Nature Climate Change* 4, no. 12 (December): 1082–1085. https://doi.org/10.1038/nclimate2410.

Tuholske, Cascade, Kelly Caylor, Chris Funk, Andrew Verdin, Stuart Sweeney, Kathryn Grace, Pete Peterson, et al. 2021. "Global Urban Population Exposure to Extreme Heat." *Proceedings of the National Academy of Sciences* 118, no. 41 (October 12, 2021): e2024792118. https://doi.org/10.1073/pnas.2024792118.

UNICEF. 2021. "The Climate Crisis is a Child Rights Crisis," August 20, 2021. https://www.unicef.org/reports/climate-crisis-child-rights-crisis.

———. 2022. *The Coldest Year of the Rest of Their Lives: Protecting Children Form the Escalating Impacts of Heatwaves.* New York: UNICEF. https://www.unicef.org/media/129506/file/UNICEF-coldest-year-heatwaves-and-children-EN.pdf.

Van Aalst, Maarten K. 2006. "The Impacts of Climate Change on the Risk of Natural Disasters." *Disasters* 30 (1): 5–18. https://doi.org/10.1111/j.1467-9523.2006.00303.x.

Xu, Zhiwei, Yang Liu, Zongwei Ma, Ghasem (Sam) Toloo, Wenbiao Hu, and Shilu Tong. 2014. "Assessment of the Temperature Effect on Childhood Diarrhea Using Satellite Imagery." *Scientific Reports* 4, no. 1 (June 23, 2014): 5389. https://doi.org/10.1038/srep05389.

Xu, Zhiwei, Perry E. Sheffield, Hong Su, Xiaoyu Wang, Yan Bi, and Shilu Tong. 2014. "The Impact of Heat Waves on Children's Health: A Systematic Review." *International Journal of Biometeorology* 58, no. 2 (March 1, 2014): 239–247. https://doi.org/10.1007/s00484-013-0655-x.

Zhou, Decheng, Shuqing Zhao, Liangxia Zhang, Ge Sun, and Yongqiang Liu. 2015. "The Footprint of Urban Heat Island Effect in China." *Scientific Reports* 5, no. 1 (June 10, 2015): 11160. https://doi.org/10.1038/srep11160.

Zivin, Joshua Graff, and Jeffrey Shrader. 2016. "Temperature Extremes, Health, and Human Capital." *The Future of Children* 26 (1): 31–50. https://doi.org/10.1353/foc.2016.0002.

Figure 1: Change in Average Share of Time at or above UTCI Thresholds for Children 1990-2020

(a) Changes between 1990 and 2020 in percentage points

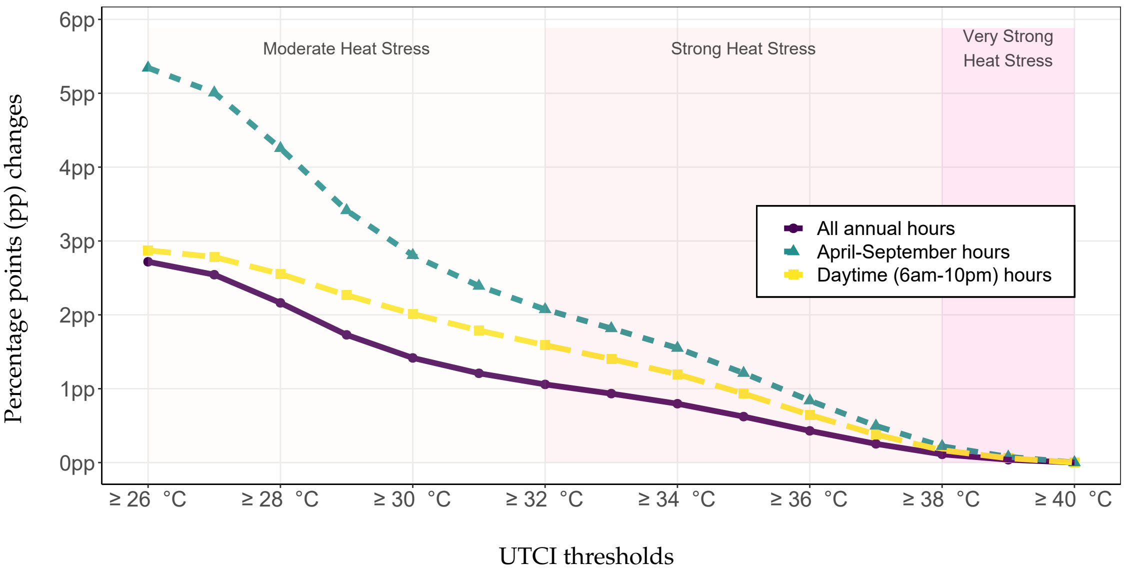

(b) Changes between 1990 and 2020 in percentage

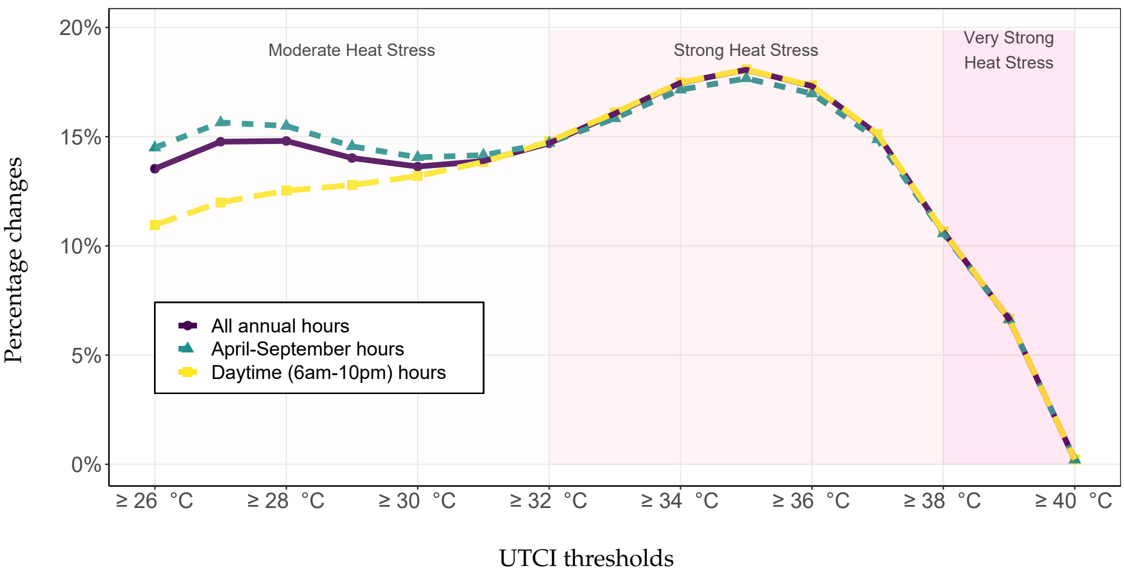

Notes: The y-axis denotes the percentage increase in hourly heat exposure for an average child in China from 1990 to 2020. The size of the circle represents the percentage point increase in hour heat exposure for an average child in China from 1990 to 2010. The circle in red shows the results when all hours are included, whereas the circle in blue shows the results when day-time hours are included. Table D.1 in Appendix documents the exact values.

Figure 2: Share of Children at Risk of Heat Stress, 1990 to 2020

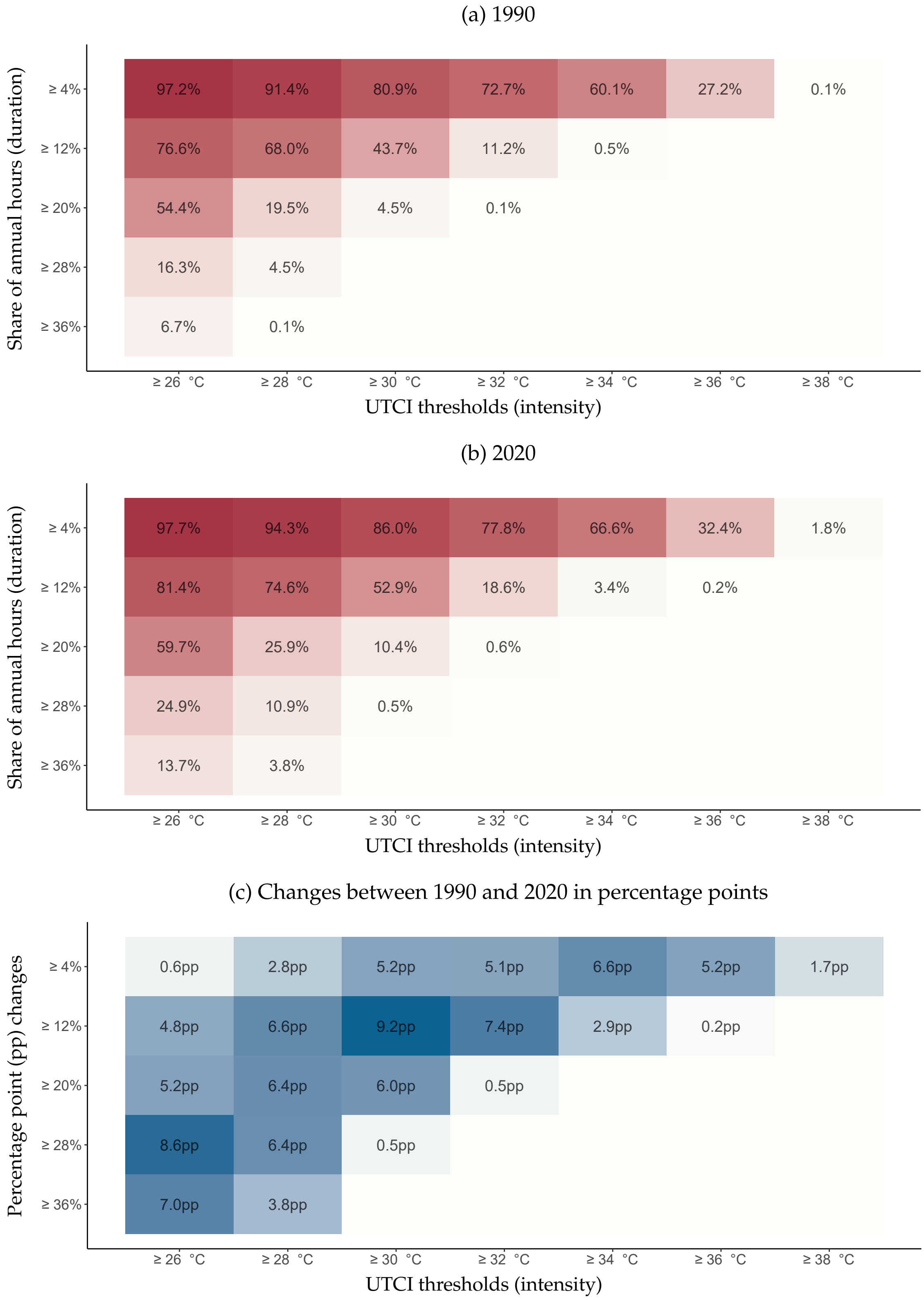

Notes: The y-axis denotes the percentage increase in hourly heat exposure for an average child in China from 1990 to 2020. The size of the circle represents the percentage point increase in hour heat exposure for an average child in China from 1990 to 2010. The circle in red shows the results when all hours are included, whereas the circle in blue shows the results when daytime hours are included. Table D.1 in Appendix documents the exact values.

Figure 3: Decomposed Change in Average Share of Time Children at Risk of Heat Stress

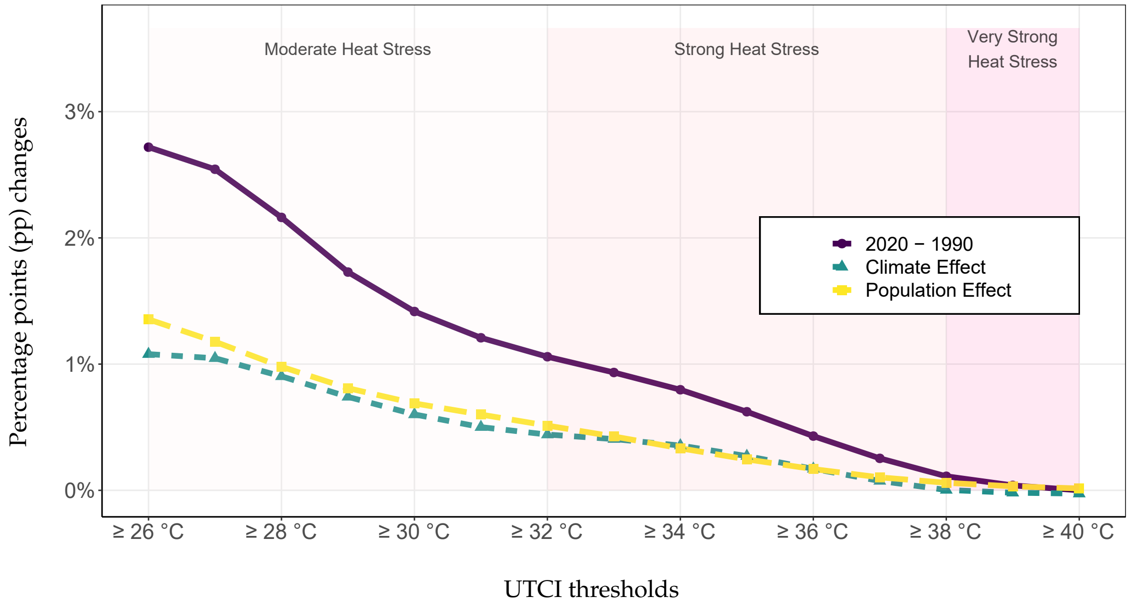

Notes: The purple solid line represents the percentage point difference in average share of time at risk of exposure to heat stress for children ages 0 to 14 between 1990 and 2020 (the year of 1990 as reference). In the first counterfactual decomposition, we use children population distribution in 1990 with the observed temperature in 2020. The green short-dash line represents the percentage difference between the decomposition results with the baseline (climte effect). In the second counterfactual decomposition, we use children population distribution in 2020 with the observed temperature in 1990. The yellow long-dash line represents the percentage difference between the decomposition results with the baseline (population effect).

Figure 4: Regional Average Share of Time at Risk of Heat Stress for Children, 1990 to 2020

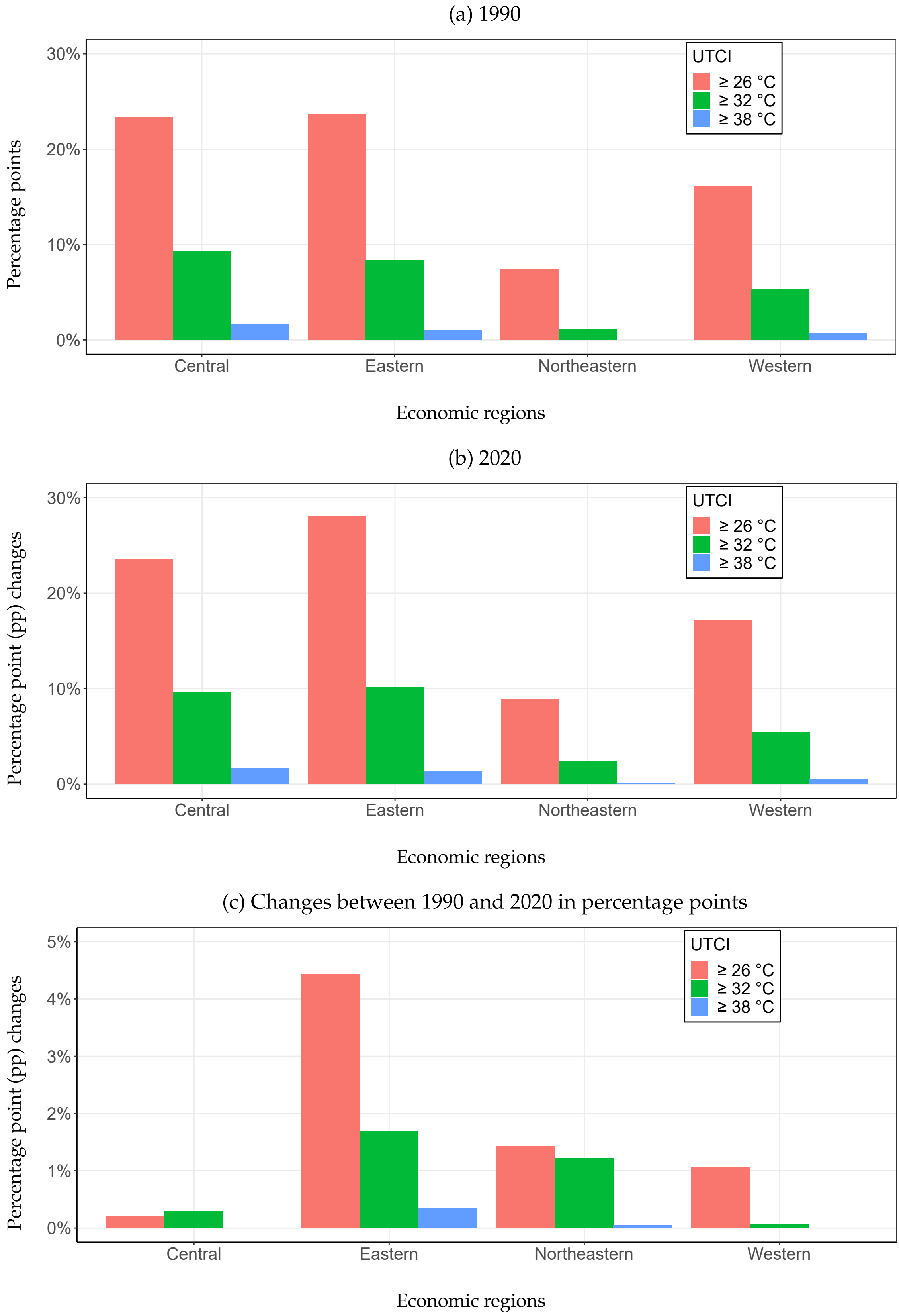

Notes: The y-axis depicts the percentage point difference from 2020 and 1990 heat exposure for children ages 0-14. We display these differences across the four economic regions of China and across different thresholds of heat exposure (moderate, strong, and very strong).

ONLINE APPENDIX

Rising Temperatures, Rising Risks: Changes in Chinese Children's Heat Exposure between1990 and 2020

Kai Feng, Marco M. Laghi, Jere R. Behrman, Emily Hannum, and Fan Wang

A Method—Population, Time, and Temperature Exposure

A.1 Framework for Analyzing Population-Heat Exposure Changes over Time

We now formalize our temperature-exposure analysis framework across time and space. Specifically, let $c_l(t)$ be the UTCI temperature experienced by an individual at a moment in time t at a location l. Between period t and $t+\tau$, the share of time that individuals at location l experience temperature $c_l(t)$ over threshold c^* is, $s_l(c^*, t, \tau)$:

$$s_l(c^*, t, \tau) = \frac{1}{\tau}\int_t^{t+\tau} \mathbf{1}\{c_l(t) > c^*\}\, dt\ . \tag{1}$$

Depending on the analysis, our definition of time period includes all time during the day, all day time hours (6 am to 10 pm), or all hours within different seasons (e.g., April–September, October–March). Additionally, let $P_{t \leqslant t < t+\tau}(l|m)$ be the share of population for socio-demographic group m in a location l, among L locations in total between time t and $t+\tau$. Total population shares across locations sum up to 1: $\sum_{l=1}^{L} P_{t \leqslant t < t+\tau}(l|m) = 1$.

We compute two key sets of statistics. First, we compute $\mathcal{S}_m(c^*, t, \tau)$, which measures, during a particular interval of time, the average share of time individuals of socio-demographic group m are exposed to temperature over threshold c^*:

$$\mathcal{S}_m(c^*, t, \tau) = \sum_{l=1}^{L} P_{t \leqslant t < t+\tau}(l|m) \cdot s_l(c^*, t, \tau)\,. \tag{2}$$

Since $\mathcal{S}_m(c^*, t, \tau)$ is a statistics for share of time, it varies between 0 and 1. In particular, $\lim_{c^* \to \infty} \mathcal{S}_m(c^*, t, \tau) = 0$ and $\lim_{c^* \to -\infty} \mathcal{S}_m(c^*, t, \tau) = 1$. A key aggregate statistic for how temperature exposure shifts between period t' and t is the following difference:

$$\Delta\mathcal{S}_{m,t',t}(c^*, \tau) = \mathcal{S}_m\left(c^*, t', \tau\right) - \mathcal{S}_m(c^*, t, \tau)\,. \tag{3}$$

$\Delta\mathcal{S}_{m,t',t}(c^*, \tau)$ is the population-weighted average increase in the share of time exposed to the potential key temperature threshold c^* between time t and t' for population group m. $\Delta\mathcal{S}_{m,t',t}(c^*, \tau)$ shifts due to both shifts in the population distribution as well as the distribution of temperature between t and t', thus taking into account both population and meteorological changes across time and space.

Second, we compute the share of individuals at risk, based on a joint consideration of the relevant temperature threshold that might be considered risky for human development, and the share of time exposed to such temperature that would put individuals at risk of non-transitory impacts. We consider these two joint dimensions of risks in computing population exposure statistics. Specifically, let $s^*(\tau)$ be a particular share-of-time threshold within span of time τ above a specific temperature risk threshold. We define the m-, c^*-, and s^*-specific at-risk measure $\mathcal{R}_m(c^*, s^*, t, \tau)$ between time t and $t+\tau$ as:

$$\mathcal{R}_m(c^*, s^*, t, \tau) = \sum_{l=1}^{L} P_{t \leqslant t < t+\tau}(l|m) \cdot \mathbf{1}\{s_l(c^*, t, \tau) > s^*(\tau)\}. \tag{4}$$

By construction, $\mathcal{R}_m(c^*, s^* = 0, t, \tau) \leqslant 1$ and $\mathcal{R}_m(c^*, s^* = 1, t, \tau) = 0$. Additionally, the share of individuals experiencing greater than s^* share of time over c^* threshold converges to 0 as c^* increases: $\lim_{c^* \to \infty} \mathcal{R}_m(c^*, s^*, t, \tau) = 0$.

For the socio-demographic group indexed by m, given temperature threshold c^* and share of time threshold s^*, the percentage increase over time in the share of individuals from this group at risk of excess heat exposure is:

$$\Delta\mathcal{R}_{m,t',t}(c^*, s^*, \tau) = \mathcal{R}_m\left(c^*, s^*, t', \tau\right) - \mathcal{R}_m(c^*, s^*, t, \tau). \tag{5}$$

One important aspect of our framework is that computing $\mathcal{R}_m(c^*, s^*, t, \tau)$ and $\Delta\mathcal{R}_{m,t',t}(c^*, s^*, \tau)$ do not require the use of harmonized geographic data overtime. This is often a constraint in the analysis of temperature changes over time, due to shifting administrative boundaries, especially across large spans of time. In our framework, we consider all $l \in \{1, \ldots, L\}$ locations within a region, and generate time-specific population-temperature cumulative distribution functions by sorting locations along the gradient of heat exposures and summing up the share of population for socio-demographic group m along ascending levels of heat exposures. While our distributions are discretized by location-level administrative units, when there are large number of locations with dispersed population, the population-temperature distributions tend to be approximately smooth. Cross time comparisons, especially at higher levels of regional aggregation, are based on these approximately smooth distributions over time. Hence moments and percentiles of these population-temperature distributions are robust to shifts in sub-region location boundaries.

A.2 Framework and Empirical Results

In our empirical application, t is 1990 and, t' is 2020, τ is one calendar year, and m is children between ages 0 and 14. Additionally, we approximate continuous time with hourly measurements. As an example, $\Delta\mathcal{R}_{\text{children},2020,1990}$ with $c^* = 28$ and $s^* = 0.1$ provides the change in the percentage points of children exposed to temperature over 28 degrees for greater than 10 percent of their time during a year.

Results for $\Delta\mathcal{S}_{m=\text{ages 0 to 15},t'=\text{year 2020},t=\text{year 1990}}(c^*, \tau = 1 \text{ year})$ are summarized in Figure 1 and Tables D.1 and D.2. These capture changes in the average share of time children are exposed to temperature over a range of heat thresholds—$23°C \leqslant c^* \leqslant 40°C$—considering all hours, day time hours, or hours during hotter and colder seasons.

Results for $\Delta\mathcal{R}_{m=\text{ages 0 to 15},t'=\text{year 2020},t=\text{year 1990}}(c^*, s^*, \tau = 1 \text{ year})$ are summarized in Figure 2 Tables D.3 and D.4. These capture changes in the share of children experiencing ambient heat exposure for over a range of c^* heat *intensity* thresholds—$23°C \leqslant c^* \leqslant 40°C$—and s^* heat exposure *duration* thresholds—4% of year $\leqslant s^* \leqslant$ 36% of year.

Additionally, Figure 3 and Tables D.5 and D.6 summarize decompositional results that compute changes in the average share of time of child exposure, but combining 1990 population distribution with 2020 heat exposure distribution, and also 1990 heat exposure distribution with 2020 population distribution. Finally, Figure 4 and Tables D.7 and D.8 provide regional results on the changes in the average share of time of child exposure.

B Data

B.1 ERA5 Data Details

ERA5-HEAT, produced by the European Centre for Medium-Range Weather Forecasts (ECMWF), represents the fifth generation of atmospheric reanalysis of global climate (Napoli 2020). Covering the period from 1940 to the present, ERA5-HEAT comprises hourly gridded maps of the Universal Thermal Climate Index (UTCI) at 0.25° × 0.25° spatial resolution. The dataset is publicly accessible through the Copernicus Climate Change Service's Climate Data Store (CDS).

As described by Bröde et al. (2012), Jendritzky, Dear, and Havenith (2012), and Jendritzky and Höppe (2017), the UTCI is a widely used index to assess the human-perceived environment based on atmospheric conditions, integrating atmospheric parameters like temperature, humidity, wind speed, and solar radiation. UTCI is expressed in degrees Celsius (°C), and it provides a measure of how cold or hot people might feel under prevailing environmental conditions. The index categorizes thermal heat stress into different classes with corresponding thresholds, which are as follows: moderate heat stress, UTCI 26°C to 32°C; strong heat stress, UTCI 32°C to 38°C; very strong heat stress, UTCI 38°C to 46°C; extreme heat stress, UTCI above 46°C;

B.2 Population data input specification

In each census year, we determine the cross-country or cross-region population distribution by considering the relative dispersion of a particular population group across counties in China for a particular census year. For our analysis of children's exposure, we focus on the age group between 0 to 14 regardless of gender.

Census 1990 We use information from 2369 geographical units at the county level nested in 31 provincial administrative units from the Tabulation on 1990 China Population Census by County. We start with the 1990 Chinese Census as it is the first to offer county-level population counts for individuals between ages 0 to 14. We only include mainland China and do not include special administrative regions. Within each county, we consider the sum of ages 0 to 14 child population across genders.

Census 2020 We use information from 2853 geographical units at the county level nested in 31 provincial administrative units from the Tabulation on 2020 China Population Census by County. We only include mainland China and dionot include special administrative regions. We again include the population counts for children between ages 0 to 14 in our analysis.

C Integrating Climatic and Population Data

All project data processing, integration, and analysis code are shared at our project repository: https://github.com/ClimateInequality/PrjCEC. In this section, we summarize key aspects of how we integrate climatic and population data to enable the analysis of changes over time in heat burden facing children. Specifically, code for generating computing population-weighted exposure statistics are included in the R folder, and integrated population-climate data outputs for each analysis included in the paper are stored in the data-res folder.

C.1 ERA5-HEAT data input specification

To capture the entire mainland China area, we employ China's far-east (135°E), far-west (53°E), far-south (4°N), and far-north (54°N) points as spatial references in our API request to extract a rectangle area that contains gridded data covering latitude and longitude coordinates that encompass mainland China from the ERA5-HEAT data. We specify all months, dates, and hours in calendar years 1990 and 2020 in our API request. After downloading coordinate-specific hourly UTCI from all dates, we consolidate them into data files by year. For example, in the 2020 data file, corresponding to each coordinate in the gridded map (data rows), we include UTCI values for all hours between January 1, 2020 to December 31, 2020 (data columns).

C.2 Population data input specification

We obtain county-level demographic data from census tabulations. In each census file, there is one unique identification number for each county-level administrative unit. Each county includes demographic data by age group and gender for the corresponding census year. The county-level shapefile for each census year provides geometries defining the boundaries of each county. The geometry information for each county—summarized by county-specific sets of polygon-bounding vertices in longitude and latitude units—is important for linking the population data with the gridded UTCI data.

The final population input consists of a data matrix. In this matrix, the first column identifies a distinct county-level administrative unit ID, while other columns store the proportion of the population between ages 0 to 14 in each county relative to the total population between ages 0 to 14 during one census year. While our focus is on children between ages 0 to 14, our approach has the flexibility to be extended to any demographic group as needed.

C.3 Specifying key files

There are three key files necessary for linking population data input and UTCI input: (1) key file that links the coordinates to counties. (2) key file that links county to province and regions. (3) key file that links population input column variables to the original labels (e.g., age groups and gender), and grouping variables for aggregation purposes (i.e., age groups 0-14, 15-64, 65+).

Coordinates to counties. We use spatial join from the "sf" package in R (Pebesma 2018) to identify coordinates from UTCI data that fall within each county boundary. Some county units are too small to include any coordinates. In this case, we use the nearest coordinate to the centroid of the county geometry. The final key file includes a list of coordinates, with each coordinate matched with the corresponding county-level administrative code in China. The county code provides linkages to the county-level population census, while the coordinates provides linkages to the gridded ERA5-HEAT data.

County to province/region. Each county code can be linked back to the province and economic regions that the county belong to. In addition to province, we can easily aggregate the county to other higher level units.

Population input columns to labels. This key file provides label names to the population input columns.

C.4 Location boundaries and population-weighted temperature distributions

As stated previously, for geo-based analysis over time, harmonizing location boundaries that may change over time is often challenging. This can be difficult to deal with when analyses use county-level boundaries, as Chinese administrative names and boundaries have changed substantially over 30 years. Our child-population based analysis does not compare each county-level unit over time, instead, we compare child-population-weighted temperature distributions using cross-county information.

Depending on our analysis, we consider all counties in China, in a region, or in a province, and generate year-specific population-temperature cumulative distribution functions by sorting counties along the gradient of heat exposures and summing up the share of child population along ascending levels of heat exposures. While our distributions are discretized by county-level administrative units, at regional and national aggregation levels, given that there are 2369 (in 1990) and 2853 (in 2020) county-level administrative units in China, the population-temperature distributions are approximately smooth. Cross time comparisons, especially at the national and regional levels, are based on these fine-grained discrete distribution.

D Additional Results on heat exposure for children

Code and results for the additional results in this section as well as in the main text of the paper are accessible at our project repository: https://github.com/ClimateInequality/PrjCEC. Specifically, code for generating the statistics shown in tables and figures are stored in the R-script folder, and code and output for visualizaing and tabularization are stored in the res folder.

1. Section D.1 and main text Figure 1 results and code:
    - Generate statistics: R-script/run_1a_mean_child_all24, R-script/run_1b_mean_child_6t22, and R-script/run_1c_mean_child_seasons
    - Tabulate and visualize: R-script/tabfig_1_mean_child
    - Tables and figures: res/res_mean_child
2. Section D.2 and main text Figure 2 results and code:
    - Generate statistics: R-script/run_2a_atrisk_child
    - Tabulate and visualize: R-script/tabfig_2_at_risk
    - Tables and figures: res/res_atrisk
3. Section D.3 and main text Figure 3 results and code:
    - Generate statistics: R-script/run_3a_decompose and R-script/run_3b_decompose_regional
    - Tabulate and visualize: R-script/tabfig_3_decompose
    - Tables and figures: res/res_decompose
4. Section D.4 and main text Figure 4 results and code:
    - Generate statistics: R-script/run_4a_mean_child_all24_by_region and R-script/run_4b_mean_child_all24_by_province
    - Tabulate and visualize: R-script/tabfig_4_region_prov
    - Tables and figures: res/res_region_prov

D.1 Average shares of time of heat exposure for children

In Tables D.1 and D.2, we present additional details on the change in average share of time at risk of exposure to heat stress thresholds for Chinese children (ages 0–14), between the years 1990 and 2020. We focus on the annual average share of time that Chinese children are exposed to UTCI temperature over thresholds $z\,^\circ$C. We group thresholds into four panels focusing on exposures to at least borderline thermal stress (23 °C–25 °C), to at least moderate heat stress (26 °C–31 °C), to at least strong heat stress (32 °C–37 °C), and to different thresholds of very strong heat exposure (38 °C–40 °C).

Table D.1's first four columns contain our main results where we consider ambient exposure during all hours of 1990 and 2020. The remaining four columns in Table D.1 present results considering only daytime (between 6 am and 10 pm) hours. Table D.2 presents results where we compare the average share of time at risk of exposure to heat stress thresholds in the warmer months of April, May, June, July, August and September with the colder months of January, February, March, October, November and December in 1990 and 2020.

What Tables D.1 and D.2 show is that the share of time at risk of exposure to heat stress thresholds for children is increasing across each threshold in which heat stress is present (i.e. moderate, strong, and very strong). Zooming further into Table D.1 and the result of 2.7 pp of increase in heat exposure $\geqslant 26\,^\circ$C, we note that this is not all due to increases in moderate heat stress. This is evidenced by there being a 1.1 pp increase in heat exposure at $\geqslant 32\,^\circ$C. Jointly these results mean that approximately 60% $\left(\frac{2.7-1.1}{2.7} \approx 0.6\right)$ of the 2.7 pp comes from increases in moderate heat exposure.

Further, in comparing the share of time differences in Tables D.1 and D.2, there are approximately 30 to 50 percent higher shares of time of children being at risk of exposure to heat stress in 2020 for daytime vs all day hours. This is a mechanical result, due to us dropping about 40 percent of the hours from the day $((24-14)/24)$. Additionally, there are between approximately 14 and 18 percent increases in shares of time at risk of exposure under Panels B and C for all hours, daytime only, as well as April-September results. October to March started in 1990 with very low levels of shares of time at risk of exposure to heat thresholds of average very strong and at strong heat stress, and then experienced very large percent increases.

Table D.1: Change in Average Share of Time at Risk of Exposure to Heat Stress Thresholds for Children, 1990 to 2020

	All annual hours ⩾ UTCI thresholds				Day time (6 am-10 pm) hours ⩾ UTCI thresholds			
	Share of time		Changes		Share of time		Changes	
UTCI thresholds	1990	2020	Level	%	1990	2020	Level	%
Panel a: Very strong heat stress								
⩾ 40 °C	0.3%	0.3%	0.0007pp	0.2%	0.4%	0.4%	0.001pp	0.2%
⩾ 39 °C	0.6%	0.6%	0.0pp	6.7%	0.9%	0.9%	0.1pp	6.7%
⩾ 38 °C	1.0%	1.2%	0.1pp	10.6%	1.6%	1.7%	0.2pp	10.7%
Panel b: At least strong heat stress								
⩾ 37 °C	1.7%	1.9%	0.3pp	15.1%	2.5%	2.9%	0.4pp	15.1%
⩾ 36 °C	2.5%	2.9%	0.4pp	17.3%	3.7%	4.4%	0.6pp	17.3%
⩾ 35 °C	3.4%	4.1%	0.6pp	18.1%	5.2%	6.1%	0.9pp	18.1%
⩾ 34 °C	4.6%	5.4%	0.8pp	17.5%	6.8%	8.0%	1.2pp	17.5%
⩾ 33 °C	5.8%	6.7%	0.9pp	16.1%	8.7%	10.1%	1.4pp	16.1%
⩾ 32 °C	7.2%	8.3%	1.1pp	14.7%	10.8%	12.3%	1.6pp	14.8%
Panel c: At least moderate heat stress								
⩾ 31 °C	8.7%	9.9%	1.2pp	13.9%	12.9%	14.7%	1.8pp	13.8%
⩾ 30 °C	10.4%	11.8%	1.4pp	13.6%	15.2%	17.3%	2.0pp	13.2%
⩾ 29 °C	12.3%	14.1%	1.7pp	14.0%	17.7%	20.0%	2.3pp	12.8%
⩾ 28 °C	14.6%	16.8%	2.2pp	14.8%	20.4%	22.9%	2.6pp	12.5%
⩾ 27 °C	17.2%	19.8%	2.5pp	14.8%	23.2%	26.0%	2.8pp	12.0%
⩾ 26 °C	20.1%	22.8%	2.7pp	13.5%	26.2%	29.1%	2.9pp	11.0%
Panel d: At least borderline thermal stress								
⩾ 25 °C	23.0%	25.7%	2.7pp	11.8%	29.3%	32.1%	2.8pp	9.7%
⩾ 24 °C	25.9%	28.6%	2.6pp	10.1%	32.3%	35.1%	2.7pp	8.5%
⩾ 23 °C	28.7%	31.3%	2.6pp	9.0%	35.3%	38.1%	2.7pp	7.7%

Note: Columns 1, 2, 5, and 6 show the annual average share of time at risk of exposure to heat stress thresholds (UTCI temperatures at $\geqslant z$ °C) for children in China (ages 0–14). Columns 3, 4, 7, and 8 show 1990 to 2020 changes in percentage points (level) or percentage (%) of the average shares of time exposed to heat. We consider both all hourly as well as only daytime hourly (between 6 am and 10 am) temperature data.

Table D.2: Change in Average Share of Time at Risk of Exposure to Heat Stress Thresholds for Children, during Warmer and Colder Months, 1990 to 2020

	April–September hours ⩾ UTCI thresholds				October–March hours ⩾ UTCI thresholds			
	Share of time		Changes		Share of time		Changes	
UTCI thresholds	1990	2020	Level	%	1990	2020	Level	%
Panel a: Very strong heat stress								
⩾ 40 °C	0.6%	0.6%	0.001pp	0.2%	0.00002%	0.00008%	0.00006pp	334.3%
⩾ 39 °C	1.2%	1.2%	0.1pp	6.6%	0.0001%	0.0004%	0.0002pp	159.0%
⩾ 38 °C	2.1%	2.3%	0.2pp	10.6%	0.0004%	0.002%	0.001pp	373.7%
Panel b: At least strong heat stress								
⩾ 37 °C	3.3%	3.8%	0.5pp	14.9%	0.002%	0.010%	0.008pp	476.0%
⩾ 36 °C	4.9%	5.8%	0.8pp	17.0%	0.006%	0.02%	0.0pp	291.4%
⩾ 35 °C	6.9%	8.1%	1.2pp	17.7%	0.02%	0.05%	0.0pp	144.1%
⩾ 34 °C	9.0%	10.6%	1.6pp	17.1%	0.06%	0.10%	0.0pp	67.0%
⩾ 33 °C	11.5%	13.3%	1.8pp	15.8%	0.1%	0.2%	0.0pp	35.1%
⩾ 32 °C	14.1%	16.2%	2.1pp	14.7%	0.3%	0.3%	0.0pp	14.1%
Panel c: At least moderate heat stress								
⩾ 31 °C	16.9%	19.3%	2.4pp	14.2%	0.5%	0.5%	0.0pp	4.2%
⩾ 30 °C	20.0%	22.8%	2.8pp	14.1%	0.8%	0.8%	0.0pp	2.5%
⩾ 29 °C	23.4%	26.9%	3.4pp	14.6%	1.2%	1.2%	0.0pp	3.0%
⩾ 28 °C	27.5%	31.7%	4.3pp	15.5%	1.7%	1.7%	0.1pp	3.4%
⩾ 27 °C	32.0%	37.0%	5.0pp	15.6%	2.4%	2.4%	0.1pp	2.8%
⩾ 26 °C	36.9%	42.2%	5.3pp	14.5%	3.2%	3.3%	0.1pp	2.5%
Panel d: At least borderline thermal stress								
⩾ 25 °C	41.7%	47.0%	5.3pp	12.7%	4.2%	4.4%	0.1pp	2.7%
⩾ 24 °C	46.3%	51.4%	5.1pp	11.0%	5.4%	5.6%	0.2pp	3.0%
⩾ 23 °C	50.6%	55.5%	4.9pp	9.7%	6.8%	7.1%	0.3pp	4.0%

Note: Columns 1, 2, 5, and 6 show the annual average share of time at risk of exposure to heat stress thresholds (UTCI temperatures at $\geqslant z$ °C) for children in China (ages 0–14). Columns 3, 4, 7, and 8 show 1990 to 2020 changes in percentage points (level) or percentage (%) of the average shares of time exposed to heat. We compare temperatures across time for April, May, June, July, August and September and then for January, February, March, October, November and December of each year. We consider all 24 hours.

D.2 Share of children at risk of heat exposure

In Tables D.3 and D.4, we present additional details from the analysis of the minimal share of children at risk of exposure to heat stress thresholds, considering the double thresholds of intensity (UTCI temperature thresholds $z\,^\circ$C) and duration (share of time in year thresholds y%). In each scenario, the share of children is computed by aggregating the share of the child population from locations (counties) experiencing these double thresholds of exposure.

In both Tables D.3 and D.4, across the columns, we present 9 duration thresholds, starting with at least 2 weeks or half a month of heat exposure (approximately 4% of a year's time) and ending with at least 18 weeks or 4.1 months (approximately 36% of a year's time) of exposure. Across the rows, we consider UTCI thresholds including a number of at least moderate and at least strong heat stress thresholds. In Table D.3, Panels A and B present shares of children at risk in 1990 and 2020. In Table D.3, Panels A and B present percentage points and percentage changes between 1990 and 2020.

In Table D.3, we show that at least some children in China during the year 1990 experienced at least some amount of moderate heat stress ($\geqslant 26\,^\circ$C) for as little as two weeks to as long as eighteen weeks: 97.2% of children and 6.7% of children respectively. By 2020, the percentage of children experiencing at least moderate heat stress increased across all weekly intervals: 97.7% and 13.7% of children respectively. The change in children experiencing at least Moderate heat stress for eighteen weeks or 36% of their year has more than doubled, as depicted in Table D.4 Panel B. Looking only two degrees higher while still within the category of moderate heat stress ($\geqslant 28\,^\circ$C), this change is even more dramatic: 3.8% of children in 2020 experienced $\geqslant 28\,^\circ$C for three months, 38 times higher than 0.1% (several hundred thousand) children in 1990.

Looking at the higher heat stress thresholds in both Table D.3 and Table D.4 Panel B, like strong heat stress ($\geqslant 32\,^\circ$C) we also show broad increases in the percentage of children exposed, although for not as many weekly time intervals in either 1990 or 2020. We estimate that for at least two weeks, 72.7% of children in China experienced at least strong heat stress ($\geqslant 32\,^\circ$C) in 1990. By 2020, this minimal strong heat stress threshold was met by 77.8% of children. While no child in either 1990 nor 2020 experienced more than ten weeks of Strong heat stress ($\geqslant 32\,^\circ$C), those ten weeks of strong heat stress or more than 20% of a year were felt by 0.1% of children in 1990 and six times as many children in 2020.

Between 1990 and 2020, the percentage of children experiencing multiple heat stress thresholds increased across new time interval thresholds. For the higher thresholds of at least moderate heat stress($\geqslant 30\,^{\circ}\mathrm{C}$), the maximum time interval where any child experienced heat stress was twelve weeks ($\geqslant$ 24% of the year), by 2020 some amount of children were experiencing sixteen weeks ($\geqslant$ 32% of the year) under at least moderate heat stress ($\geqslant 30\,^{\circ}\mathrm{C}$). In the middle and higher ends of at least strong heat stress ($\geqslant 34\,^{\circ}\mathrm{C}$ and $\geqslant 36\,^{\circ}\mathrm{C}$), the maximum amount of time children experienced these levels of heat stress rose from eight to ten weeks, and four to six weeks ($\geqslant$ 8% to $\geqslant$ 12% of the year) respectively. Finally, at very strong heat stress ($\geqslant 38\,^{\circ}\mathrm{C}$), the same percentage of children that experienced the maximum time interval of two weeks ($\geqslant$ 4% of the year) in 1990, then reached a new maximum time interval in 2020 of four weeks of exposure ($\geqslant$ 8% of the year).

Table D.3: Share of Children at Risk of Exposure to Heat Stress Thresholds, 1990 to 2020

	Minimal share of time in year thresholds and corresponding number of weeks								
	$\geqslant 4\%$	$\geqslant 8\%$	$\geqslant 12\%$	$\geqslant 16\%$	$\geqslant 20\%$	$\geqslant 24\%$	$\geqslant 28\%$	$\geqslant 32\%$	$\geqslant 36\%$
UTCI thresholds	2 weeks	4 weeks	6 weeks	8 weeks	10 wks	12 wks	14 wks	16 wks	18 wks
Panel a: 1990									
$x\%$ (cell) of children with at least $y\%$ (column) of time in year 1990 at $\geqslant z$ °C (row) heat threshold									
Very strong heat stress									
$\geqslant 38$ °C	0.1%								
At least strong heat stress									
$\geqslant 36$ °C	27.2%	0.1%							
$\geqslant 34$ °C	60.1%	15.1%	0.5%						
$\geqslant 32$ °C	72.7%	52.1%	11.2%	1.4%	0.1%				
At least moderate heat stress									
$\geqslant 30$ °C	80.9%	69.0%	43.7%	13.1%	4.5%	0.4%			
$\geqslant 28$ °C	91.4%	77.5%	68.0%	44.6%	19.5%	7.5%	4.5%	1.4%	0.1%
$\geqslant 26$ °C	97.2%	87.0%	76.6%	68.5%	54.4%	31.1%	16.3%	8.6%	6.7%
At least borderline thermal stress									
$\geqslant 24$ °C	98.8%	96.0%	84.9%	76.6%	70.8%	63.2%	44.2%	25.3%	13.9%
Panel b: 2020									
$x\%$ (cell) of children with at least $y\%$ (column) of time in year 2020 at $\geqslant z$ °C (row) heat threshold									
Very strong heat stress									
$\geqslant 38$ °C	1.8%	0.1%							
At least strong heat stress									
$\geqslant 36$ °C	32.4%	2.1%	0.2%						
$\geqslant 34$ °C	66.6%	20.1%	3.4%	0.4%					
$\geqslant 32$ °C	77.8%	59.1%	18.6%	6.1%	0.6%				
At least moderate heat stress									
$\geqslant 30$ °C	86.0%	75.6%	52.9%	20.7%	10.4%	3.0%	0.5%	0.1%	
$\geqslant 28$ °C	94.3%	83.5%	74.6%	53.6%	25.9%	17.4%	10.9%	7.4%	3.8%
$\geqslant 26$ °C	97.7%	91.9%	81.4%	74.5%	59.7%	34.8%	24.9%	17.9%	13.7%
At least borderline thermal stress									
$\geqslant 24$ °C	98.7%	97.0%	89.7%	81.2%	76.4%	65.6%	45.1%	32.4%	23.3%

Note: Cells show the shares of Chinese children (ages 0–14) experiencing at least $y\%$ of their time in a year at risk of exposure to at least a particular z °C UTCI temperature threshold. Shares of children at risk are computed based on aggregating population shares from locations (counties) experiencing the various combinations of heat stress duration (share of time) and intensity (temperature) thresholds. For minimal shares of time in a year, the correspondence between the share of time and the number of weeks is based on the fact that the average of N weeks of time and $\frac{N}{4}$ months of time is approximately $(N \cdot 2)\%$ of total share of time in a year. To enhance contrast, values are rounded and cells with values less than 0.05% or 0.05pp are left empty. We consider all 24 hours and 12 months.

Table D.4: Change in Share of Children at Risk of Exposure to Heat Stress Thresholds, 2020-1990

	Minimal share of time in year thresholds and corresponding number of weeks								
	⩾ 4%	⩾ 8%	⩾ 12%	⩾ 16%	⩾ 20%	⩾ 24%	⩾ 28%	⩾ 32%	⩾ 36%
UTCI thresholds	2 weeks	4 weeks	6 weeks	8 weeks	10 wks	12 wks	14 wks	16 wks	18 wks
Panel a: 2020% − 1990%									
Increases in percentage points (cell) of children with at least y% (column) of time at ⩾ z °C (row) heat threshold									
Very strong heat stress									
⩾ 38 °C	1.7pp	0.1pp							
At least strong heat stress									
⩾ 36 °C	5.2pp	2.0pp	0.2pp						
⩾ 34 °C	6.6pp	5.0pp	2.9pp	0.4pp					
⩾ 32 °C	5.1pp	6.9pp	7.4pp	4.7pp	0.5pp				
At least moderate heat stress									
⩾ 30 °C	5.2pp	6.5pp	9.2pp	7.6pp	6.0pp	2.6pp	0.5pp	0.1pp	
⩾ 28 °C	2.8pp	6.0pp	6.6pp	8.9pp	6.4pp	9.9pp	6.4pp	6.0pp	3.8pp
⩾ 26 °C	0.6pp	5.0pp	4.8pp	6.0pp	5.2pp	3.7pp	8.6pp	9.3pp	7.0pp
At least borderline thermal stress									
⩾ 24 °C	-0.2pp	1.0pp	4.8pp	4.6pp	5.5pp	2.5pp	0.9pp	7.2pp	9.4pp
Panel b: $\frac{2020\% - 1990\%}{1990\%} \cdot 100$									
Percentage increases (cell) of children with at least y% (column) of time at ⩾ z °C (row) heat threshold									
Very strong heat stress									
⩾ 38 °C	1.8k%								
At least strong heat stress									
⩾ 36 °C	19.2%	2.3k%							
⩾ 34 °C	10.9%	33.1%	606%						
⩾ 32 °C	7.0%	13.3%	66.3%	330%	792%				
At least moderate heat stress									
⩾ 30 °C	6.4%	9.4%	20.9%	58.5%	133%	654%			
⩾ 28 °C	3.1%	7.7%	9.7%	20.0%	32.9%	131%	141%	414%	5.2k%
⩾ 26 °C	0.6%	5.7%	6.3%	8.7%	9.6%	11.7%	52.9%	109%	106%
At least borderline thermal stress									
⩾ 24 °C	-0.2%	1.0%	5.7%	6.0%	7.8%	3.9%	2.1%	28.5%	67.5%

Note: Cells show changes between 1990 and 2020 in percentage points (Panel A) and percentage (Panel B) of the shares of Chinese children (ages 0–14) experiencing at least y% of their time in a year at risk of exposure to at least a particular z °C UTCI temperature threshold. Shares of children at risk are computed based on aggregating population shares from locations (counties) experiencing the various combinations of heat stress duration (share of time) and intensity (temperature) thresholds. For minimal shares of time in a year, the correspondence between the share of time and the number of weeks is based on the fact that the average of N weeks of time and $\frac{N}{4}$ months of time is approximately $(N \cdot 2)$% of total share of time in a year. To enhance contrast, values are rounded and cells with values less than 0.05% or 0.05pp are left empty. We consider all 24 hours and 12 months.

D.3 Decomposition shifting only population or temperature distributions

In this section, we provide more details on the relative contributions of shifts in the child population distribution and the temperature distribution to overall changes in average share time exposed to heat. Our decomposition analysis is statistical in nature: we shift one distribution while holding the other constant and do not model mechanisms of change. Also note that actual changes unexplained by the sum of population and temperature decompositions are attributable to population and temperature interactions.

Following Table D.1, columns 1–3 of Table D.5 include actual annual average shares of time that children risk exposure to UTCI temperatures at $\geqslant z$ °C and percentage points changes over time. In columns 4–6, we compute exposures using the 1990 population distribution jointly with the 2020 UTCI temperature distribution. In columns 7–9, we consider exposures if the 2020 population distribution faced the 1990 UTCI temperature distribution. We present in Panel A national results. Panels B and C show results in the Eastern and Northeastern regions which experienced large increases in heat exposure (see Table D.7).

In Table D.5 we show the importance of noting population shifts alongside temperature effects. For at least strong ($\geqslant$ 32 °C) heat stress levels, child population distribution shifts nationally account for 48% (and 29% in the Eastern and 9% in the Northeastern region) and 50% (38%/16%) of at least moderate heat stress ($\geqslant$ 26 °C) change, respectively. In contrast, temperature distribution shifts account for 42% (61%/92%) and 40% (51%/81%) of the heat exposure changes, respectively. For Central and Western regions of China in Panels A and B Table D.6, population effects are less consistently greater than temperature effects, only being greater in Western China at strong ($\geqslant$ 32 °C) heat stress levels (68% versus 54%), and at higher strong heat stress thresholds ($\geqslant$ 36 °C) (27% versus -33%)

Second, we observe the importance of cross-regional movement in Tables D.5 and D.6 for at least moderate heat stress ($\geqslant$ 26 °C) on the National, Eastern , Northeastern, Central, and Western regions, where population shifts account for 50%, 38%, 16%, 21%, and -326% of the actual exposure shifts in their respective geographies. The national results are due to shifts within and across regions, whereas the regional results are attributed to only within-region shifts.

Finally, in the last column of Tables D.5 and D.6 we note the decreased importance of population effects at higher UTCI thresholds. Contribution of population distribution generally decreases with increasing heat stress thresholds: nationally (in Eastern/Northeastern/Western regions) from 61% (53%/20%/2,174,605%) at borderline heat stress of $\geqslant$ 24 °C to 39% (19%/5%/49%) at higher levels of strong heat stress $\geqslant$ 36 °C. Increases in the higher heat exposures come more from increasing temperatures rather than from populations moving to locations that were already hotter in 1990.

Table D.5: Decompose changes in average share of time exposed to heat

	Actual 2020 vs 1990			2020 UTCI with 1990 population			1990 UTCI with 2020 population		
	Share of time		Changes	Share-time	Decompose changes		Share-time	Decompose changes	
UTCI thresholds	1990	2020	Δ	Prediction	Vs. 1990	% of Δ	Prediction	Vs. 1990	% of Δ
Panel A: National									
At least strong heat stress									
$\geqslant 36\,^\circ$C	2.5%	2.9%	0.43pp	2.7%	0.17pp	40%	2.7%	0.17pp	39%
$\geqslant 34\,^\circ$C	4.6%	5.4%	0.80pp	4.9%	0.35pp	45%	4.9%	0.33pp	42%
$\geqslant 32\,^\circ$C	7.2%	8.3%	1.06pp	7.6%	0.44pp	42%	7.7%	0.51pp	48%
At least moderate heat stress									
$\geqslant 30\,^\circ$C	10.4%	11.8%	1.42pp	11.0%	0.60pp	42%	11.1%	0.69pp	49%
$\geqslant 28\,^\circ$C	14.6%	16.8%	2.16pp	15.5%	0.90pp	42%	15.6%	0.98pp	45%
$\geqslant 26\,^\circ$C	20.1%	22.8%	2.72pp	21.2%	1.08pp	40%	21.4%	1.35pp	50%
At least borderline thermal stress									
$\geqslant 24\,^\circ$C	25.9%	28.6%	2.63pp	26.8%	0.88pp	33%	27.5%	1.60pp	61%
Panel B: Eastern region									
At least strong heat stress									
$\geqslant 36\,^\circ$C	2.7%	3.5%	0.85pp	3.3%	0.59pp	70%	2.9%	0.16pp	19%
$\geqslant 34\,^\circ$C	5.3%	6.6%	1.35pp	6.1%	0.89pp	66%	5.6%	0.31pp	23%
$\geqslant 32\,^\circ$C	8.4%	10.1%	1.70pp	9.5%	1.03pp	61%	8.9%	0.50pp	29%
At least moderate heat stress									
$\geqslant 30\,^\circ$C	12.1%	14.3%	2.26pp	13.4%	1.33pp	59%	12.8%	0.73pp	32%
$\geqslant 28\,^\circ$C	17.0%	20.7%	3.70pp	19.0%	2.02pp	55%	18.2%	1.18pp	32%
$\geqslant 26\,^\circ$C	23.6%	28.1%	4.44pp	25.9%	2.27pp	51%	25.3%	1.69pp	38%
At least borderline thermal stress									
$\geqslant 24\,^\circ$C	30.6%	34.2%	3.54pp	32.0%	1.36pp	38%	32.5%	1.87pp	53%
Panel C: Northeastern region									
At least strong heat stress									
$\geqslant 36\,^\circ$C	0.04%	0.3%	0.27pp	0.3%	0.24pp	89%	0.05%	0.01pp	5%
$\geqslant 34\,^\circ$C	0.3%	1.1%	0.79pp	1.%	0.72pp	91%	0.3%	0.05pp	6%
$\geqslant 32\,^\circ$C	1.1%	2.4%	1.22pp	2.3%	1.12pp	92%	1.3%	0.11pp	9%
At least moderate heat stress									
$\geqslant 30\,^\circ$C	2.8%	4.1%	1.35pp	4.0%	1.23pp	91%	2.9%	0.17pp	13%
$\geqslant 28\,^\circ$C	5.0%	6.4%	1.39pp	6.2%	1.21pp	87%	5.2%	0.21pp	15%
$\geqslant 26\,^\circ$C	7.5%	8.9%	1.43pp	8.7%	1.16pp	81%	7.7%	0.24pp	16%
At least borderline thermal stress									
$\geqslant 24\,^\circ$C	10.4%	11.8%	1.45pp	11.4%	1.06pp	73%	10.7%	0.29pp	20%

Note: Columns (cols) 1–3 include actual annual average share of time that children in China (ages 0–14) are at risk of exposure to UTCI temperatures at $\geqslant z\ ^\circ$C (same information as cols 1–3 in Table D.1). Cols 4–6 consider heat exposure if the 1990 population distribution faced the 2020 UTCI temperature distribution. Cols 7–9 consider exposure if 2020 population faced 1990 UTCI temperatures. Cols 4 and 7 show predictions of annual average shares of time exposed to heat thresholds given decomposition scenarios. Cols 5 and 8 show differences between predictions and 1990 actual average shares. Cols 6 and 9 show the share of column 3 actual changes that the predictions from cols 5 and 8 account for. See Table D.7 for provincial-level administrative units in the Eastern and Northeastern regions. We consider all 24 hours and 12 months.

Table D.6: Decompose changes in average share of time exposed to heat

	Actual 2020 vs 1990			2020 UTCI with 1990 population			1990 UTCI with 2020 population		
	Share of time		Changes	Share-time	Decompose changes		Share-time	Decompose changes	
UTCI thresholds	1990	2020	Δ	Prediction	Vs. 1990	% of Δ	Prediction	Vs. 1990	% of Δ
Panel A: Central region									
At least strong heat stress									
$\geqslant 36\,^\circ$C	3.7%	3.7%	0.08pp	3.6%	-0.03pp	-33%	3.7%	0.02pp	27%
$\geqslant 34\,^\circ$C	6.2%	6.5%	0.25pp	6.4%	0.11pp	45%	6.3%	0.03pp	14%
$\geqslant 32\,^\circ$C	9.3%	9.6%	0.30pp	9.4%	0.13pp	43%	9.3%	0.04pp	14%
At least moderate heat stress									
$\geqslant 30\,^\circ$C	12.9%	13.3%	0.39pp	13.1%	0.21pp	53%	12.9%	0.04pp	10%
$\geqslant 28\,^\circ$C	17.6%	17.9%	0.38pp	17.8%	0.19pp	51%	17.6%	0.03pp	9%
$\geqslant 26\,^\circ$C	23.4%	23.6%	0.21pp	23.4%	0.04pp	22%	23.4%	0.04pp	21%
At least borderline thermal stress									
$\geqslant 24\,^\circ$C	29.2%	29.6%	0.42pp	29.5%	0.27pp	64%	29.3%	0.08pp	19%
Panel B: Western region									
At least strong heat stress									
$\geqslant 36\,^\circ$C	1.7%	1.7%	-0.04pp	1.6%	-0.12pp	284%	1.7%	0.05pp	-112%
$\geqslant 34\,^\circ$C	3.2%	3.3%	0.03pp	3.2%	-0.09pp	-312%	3.4%	0.10pp	345%
$\geqslant 32\,^\circ$C	5.4%	5.4%	0.07pp	5.3%	-0.09pp	-133%	5.5%	0.16pp	247%
At least moderate heat stress									
$\geqslant 30\,^\circ$C	8.0%	8.2%	0.19pp	8.1%	0.01pp	7%	8.2%	0.19pp	102%
$\geqslant 28\,^\circ$C	11.5%	12.1%	0.52pp	11.8%	0.29pp	55%	11.8%	0.24pp	47%
$\geqslant 26\,^\circ$C	16.2%	17.2%	1.06pp	16.9%	0.77pp	73%	16.5%	0.30pp	28%
At least borderline thermal stress									
$\geqslant 24\,^\circ$C	21.5%	22.7%	1.13pp	22.4%	0.91pp	81%	21.8%	0.30pp	26%

Note: Columns (cols) 1–3 include actual annual average share of time that children in China (ages 0–14) are at risk of exposure to UTCI temperatures at $\geqslant z\,^\circ$C (same information as cols 1–3 in Table D.1). Cols 4–6 consider heat exposure if the 1990 population distribution faced the 2020 UTCI temperature distribution. Cols 7–9 consider exposure if 2020 population faced 1990 UTCI temperatures. Cols 4 and 7 show predictions of annual average shares of time exposed to heat thresholds given decomposition scenarios. Cols 5 and 8 show differences between predictions and 1990 actual average shares. Cols 6 and 9 show the share of column 3 actual changes that the predictions from cols 5 and 8 account for. See Table D.7 for provincial-level administrative units in the Eastern and Northeastern regions. We consider all 24 hours and 12 months.

D.4 Additional regional analysis

In this section, we augment the region-specific heat exposure analysis with province-specific analysis as well. Similar to Table D.7, we analyze changes in the average share of time at risk of heat exposure between 1990 and 2020 for Chinese children (ages 0-14). Overall national, regional, and provincial changes are due to shifts over time in both the temperature distribution and the child population distribution across space within the country, region, or province. Sub-national analyses not only show which areas are experiencing greater changes in heat exposures but also shed light on whether aggregate national and regional changes are due to population shifts across regions and across provinces within-region, respectively. [D.1]

In Panel A of Tables D.7 and D.8, we conduct our analysis based on changes in the distribution of children and temperature within each of the four economic regions of China. In successive panels, we present province-specific results based on within-province changes. Table D.7 presents results for at least Strong ($\geqslant 32\,^{\circ}$C and $\geqslant 35\,^{\circ}$C) and Very Strong heat stress ($\geqslant 38\,^{\circ}$C) exposure thresholds across columns. Table D.8 focuses on moderate ($\geqslant 26\,^{\circ}$C and $\geqslant 29\,^{\circ}$C) heat stress thresholds and also provides results for the $\geqslant 23^{\circ}$C threshold.

In Panel A of Tables D.7 and D.8 we show that in 1990, the Central region, followed by the Eastern, had the highest average share of child heat exposure time. Between 1990 and 2020, while Central exposure stagnated with 1% to 4% increases (for at least moderate and strong heat stress thresholds), the Eastern region experienced increases of 20% to 35% across heat stress thresholds, catching up to the central region. In 2020, the average Eastern region child experienced 28.1% and 10.1% of her time under at least moderate ($\geqslant 26\,^{\circ}$C) and at least strong ($\geqslant 32\,^{\circ}$C) heat stress. Meanwhile, the Northeastern region had very low average child heat exposure in 1990, but by 2020, experienced increases of 19% ($\geqslant 26\,^{\circ}$C) and 36% ($\geqslant 29\,^{\circ}$C) for average at least moderate heat stress and 106% ($\geqslant 32\,^{\circ}$C) and 457% ($\geqslant 35\,^{\circ}$C) for at least strong heat stress. In 2020, the average Northeastern region child experienced 8.9% and 2.4% of her time under at least moderate ($\geqslant 26\,^{\circ}$C) and at least strong ($\geqslant 32\,^{\circ}$C) heat stress, which are still much lower than average exposure levels in Central and Eastern regions.

In Panels B-D of Tables D.7 and D.8 we observe different levels of temperature exposure for children across provinces within the regions of China. In 2020, Hainan (Eastern), Guangdong (Eastern), Guangxi (Western), Jiangxi (Central), and Fujian (Eastern) are generally ranked from

D.1. In an extreme scenario, there might be no changes in temperatures and no changes in the distribution of population within regions, but if the overall national population shares in higher heat stress regions increase, average national child heat exposure will increase.

top 1 to 5 in terms of the average share of child time exposed to heat across all UTCI thresholds. Specifically, in 2020, children in Hainan, Guangdong, Guangxi, Jiangxi and Fujian had on average 19.2%, 15.2%, 13.2%, 12.8%, and 11.8% share of time exposed to at least strong heat stress ($\geqslant 32\,^{\circ}\mathrm{C}$), which represented respective increases of 17%, 20%, 8%, 16%, and 54% in share of time exposed compared to 1990.

On the opposite end of Panels B-D of Tables D.7 and D.8, we also observe some cases of decreasing heat exposure. While Northeastern and Eastern provinces (excluding Jiangsu) experienced substantial increases in heat exposure, provinces in Central and Western regions experienced limited exposure increases and reductions. In particular, Central China's provinces of Hubei and Anhui and Western China's provinces of Shaanxi and Sichuan generally experienced reductions in average child heat exposures across UTCI thresholds. Additionally, children in Qinghai and Xizang (Tibet) in the Western region continue to have generally no exposure to at least moderate heat stress.

Lastly, we note the extent to which provinces have similar changes in exposure. For at least strong heat stress ($\geqslant 32\,^{\circ}\mathrm{C}$), Hebei and Zhejiang in the Eastern region, along with all Northeastern provinces, all experienced between 1.0 to 1.3 percentage points increases in the average share of time heat exposure. Since the Northeastern provinces started at much lower levels, the percentage increases in the Northeastern provinces are 3 to 15 times larger. Due to heterogeneities across provinces in prior exposure levels, the same percentage points increases represented a much bigger change from the status quo for the Northeastern provinces. Other nuance is also notable in comparing provinces. In 2020, the average child experienced 7.6% and 7.8% of her annual time with at least strong heat stress ($\geqslant 32\,^{\circ}\mathrm{C}$) in the Eastern provinces of Hebei and Jiangsu, respectively. But Hebei and Jiangsu experienced a 17% increase and an 11% reduction in heat exposure between 1990 and 2020, respectively. Depending on prior exposure levels, provinces might require different types of societal and physical adjustments despite having the same level of heat exposure today.

D.4.1 Very Strong and Strong heat stress across regions

Table D.7: Regional Average Share of Time at Risk of Exposure to Strong and Very Strong Heat Stress Thresholds for Children (ages 0-14), 1990 to 2020

	At least strong heat stress								Very strong heat stress			
	⩾ UTCI 32° C				⩾ UTCI 35° C				⩾ UTCI 38° C			
	Share of time		Changes		Share of time		Changes		Share of time		Changes	
Location	1990	2020	Level	%	1990	2020	Level	%	1990	2020	Level	%
Panel A: Regions												
Eastern	8.4%	10.1%	1.7pp	20%	3.9%	5.0%	1.1pp	29%	1.0%	1.4%	0.4pp	35%
Northeastern	1.1%	2.4%	1.2pp	106%	0.1%	0.6%	0.5pp	457%	0.0%	0.1%	0.1pp	7.4k%
Central	9.3%	9.6%	0.3pp	3%	4.9%	5.1%	0.2pp	4%	1.7%	1.6%	-0.1pp	-3%
Western	5.4%	5.4%	0.1pp	1%	2.4%	2.4%	0.0pp	0%	0.7%	0.6%	-0.1pp	-18%
Panel B: Eastern region												
Beijing	2.9%	6.3%	3.4pp	117%	0.5%	2.8%	2.3pp	424%	0.0%	0.6%	0.6pp	1.2k%
Fujian	7.7%	11.8%	4.1pp	54%	2.9%	5.6%	2.7pp	94%	0.5%	1.3%	0.9pp	175%
Guangdong	12.7%	15.2%	2.5pp	20%	5.7%	7.5%	1.8pp	31%	1.3%	2.0%	0.7pp	56%
Hainan	16.3%	19.2%	2.8pp	17%	6.4%	10.0%	3.6pp	57%	0.9%	3.4%	2.4pp	261%
Hebei	6.5%	7.6%	1.1pp	17%	2.9%	3.9%	1.0pp	34%	0.8%	1.0%	0.2pp	31%
Jiangsu	8.7%	7.8%	-0.9pp	-11%	4.7%	3.8%	-0.9pp	-20%	1.7%	1.3%	-0.4pp	-25%
Shandong	6.8%	7.1%	0.4pp	6%	2.9%	3.3%	0.4pp	13%	0.5%	0.9%	0.3pp	58%
Shanghai	6.8%	6.1%	-0.7pp	-10%	3.1%	2.7%	-0.4pp	-14%	1.0%	0.6%	-0.4pp	-40%
Tianjin	5.6%	7.3%	1.7pp	31%	2.1%	3.8%	1.7pp	84%	0.2%	0.9%	0.7pp	308%
Zhejiang	8.2%	9.2%	1.0pp	12%	4.6%	4.9%	0.4pp	8%	1.9%	1.6%	-0.3pp	-14%
Panel C: Northeastern region												
Heilongjiang	0.6%	1.7%	1.1pp	175%	0.0%	0.4%	0.4pp	1.6k%	0.0%	0.0%	0.0pp	
Jilin	0.8%	2.1%	1.3pp	148%	0.0%	0.5%	0.5pp	2.7k%	0.0%	0.0%	0.0pp	
Liaoning	1.9%	2.9%	1.1pp	56%	0.3%	0.8%	0.6pp	216%	0.0%	0.1%	0.1pp	4.5k%
Panel D: Central region												
Anhui	10.1%	9.3%	-0.8pp	-7%	5.8%	5.0%	-0.9pp	-15%	2.2%	1.8%	-0.4pp	-18%
Henan	8.9%	9.5%	0.6pp	7%	4.5%	5.1%	0.5pp	12%	1.4%	1.6%	0.2pp	13%
Hubei	10.2%	9.3%	-0.9pp	-9%	5.5%	4.9%	-0.6pp	-10%	2.0%	1.3%	-0.7pp	-35%
Hunan	10.2%	10.6%	0.4pp	4%	5.0%	5.4%	0.4pp	7%	1.6%	1.6%	0.0pp	0%
Jiangxi	11.0%	12.8%	1.8pp	16%	6.1%	7.4%	1.2pp	20%	2.4%	2.9%	0.5pp	19%
Shanxi	2.6%	2.8%	0.1pp	5%	0.8%	0.7%	-0.1pp	-18%	0.2%	0.1%	-0.1pp	-53%
Panel E: Western region												
Gansu	0.8%	0.8%	0.0pp	-1%	0.1%	0.1%	0.0pp	-17%	0.0%	0.0%	0.0pp	-17%
Guangxi	12.3%	13.2%	1.0pp	8%	5.5%	6.6%	1.1pp	20%	1.5%	1.4%	-0.1pp	-7%
Guizhou	2.8%	2.1%	-0.7pp	-26%	0.7%	0.3%	-0.4pp	-53%	0.1%	0.0%	0.0pp	-54%
Neimenggu	0.9%	2.0%	1.1pp	116%	0.1%	0.6%	0.4pp	296%	0.0%	0.1%	0.1pp	268%

Continued on next page

Table D.7: Regional Average Share of Time at Risk of Exposure to Strong and Very Strong Heat Stress Thresholds for Children (ages 0-14), 1990 to 2020

	At least strong heat stress								Very strong heat stress			
	⩾ UTCI 32° C				⩾ UTCI 35° C				⩾ UTCI 38° C			
	Share of time		Changes		Share of time		Changes		Share of time		Changes	
Location	1990	2020	Level	%	1990	2020	Level	%	1990	2020	Level	%
Ningxia	2.1%	2.8%	0.7pp	31%	0.7%	0.9%	0.2pp	35%	0.1%	0.1%	0.0pp	17%
Qinghai	0.0%	0.0%	0.0pp		0.0%	0.0%	0.0pp		0.0%	0.0%	0.0pp	
Shaanxi	4.6%	4.3%	-0.4pp	-8%	1.9%	1.5%	-0.4pp	-23%	0.6%	0.2%	-0.3pp	-58%
Sichuan	8.0%	7.4%	-0.7pp	-8%	4.2%	3.6%	-0.6pp	-14%	1.3%	1.0%	-0.3pp	-23%
Xinjiang	4.3%	5.2%	0.9pp	22%	2.0%	2.4%	0.4pp	19%	0.7%	0.7%	0.0pp	0%
Xizang	0.0%	0.0%	0.0pp		0.0%	0.0%	0.0pp		0.0%	0.0%	0.0pp	
Yunnan	0.9%	1.2%	0.3pp	33%	0.1%	0.1%	0.0pp	53%	0.0%	0.0%	0.0pp	-7%

Note: We present similar statistics as in Table D.1, but now compute exposures separately for four economic regions and provincial-level administrative units in China. Columns (cols) 1–3 and 4–6 focus on at least strong UTCI heat exposure at $\geqslant$ 32 °C and $\geqslant$ 35 °C, respectively. Cols 7–9 focus on very strong UTCI heat exposure at $\geqslant$ 38 °C. Cols 1 and 2, 5 and 6, and 9 and 10 show the annual average share of time at risk of exposure to heat stress thresholds (UTCI temperatures at $\geqslant z$ °C) for children in China (ages 0–14). Cols 3 and 4, 7 and 8, and 11 and 12 show 1990 to 2020 changes in percentage points (level) or percentage (%) of the average shares of time exposed to heat. Cells are empty for percentage changes when the denominator is equal to zero. We consider all 24 hours and 12 months.

D.4.2 Moderate and No Heat Stress across regions

Table D.8: Regional Average Share of Time at Risk of Exposure to Moderate Heat Stress Thresholds for Children (ages 0-14), 1990 to 2020

	At least borderline thermal stress				At least moderate heat stress							
	⩾ UTCI 23° C				⩾ UTCI 26° C				⩾ UTCI 29° C			
	Share of time		Changes		Share of time		Changes		Share of time		Changes	
Location	1990	2020	Level	%	1990	2020	Level	%	1990	2020	Level	%
Panel A: Regions												
Eastern	33.8%	37.0%	3.2pp	9%	23.6%	28.1%	4.4pp	19%	14.3%	17.1%	2.8pp	20%
Northeastern	12.0%	13.5%	1.5pp	13%	7.5%	8.9%	1.4pp	19%	3.8%	5.2%	1.4pp	36%
Central	32.0%	32.7%	0.7pp	2%	23.4%	23.6%	0.2pp	1%	15.1%	15.5%	0.4pp	3%
Western	24.3%	25.3%	1.0pp	4%	16.2%	17.2%	1.1pp	7%	9.7%	10.0%	0.3pp	3%
Panel B: Eastern region												
Beijing	19.0%	23.2%	4.3pp	23%	12.1%	16.2%	4.1pp	34%	7.0%	10.7%	3.7pp	53%
Fujian	38.9%	45.6%	6.7pp	17%	24.6%	32.5%	7.9pp	32%	14.1%	19.0%	4.9pp	35%
Guangdong	51.9%	55.5%	3.7pp	7%	37.5%	45.3%	7.8pp	21%	21.6%	26.3%	4.7pp	22%
Hainan	63.5%	63.4%	0.0pp	0%	47.1%	51.8%	4.7pp	10%	27.7%	31.5%	3.9pp	14%
Hebei	24.4%	25.1%	0.7pp	3%	17.0%	18.0%	1.0pp	6%	10.8%	12.3%	1.5pp	14%
Jiangsu	30.5%	29.7%	-0.8pp	-3%	22.5%	21.5%	-1.0pp	-4%	14.3%	13.7%	-0.6pp	-4%

Continued on next page

Table D.8: Regional Average Share of Time at Risk of Exposure to Moderate Heat Stress Thresholds for Children (ages 0-14), 1990 to 2020

	At least borderline thermal stress				At least moderate heat stress							
	$\geqslant$ UTCI 23° C				$\geqslant$ UTCI 26° C				$\geqslant$ UTCI 29° C			
	Share of time		Changes		Share of time		Changes		Share of time		Changes	
Location	1990	2020	Level	%	1990	2020	Level	%	1990	2020	Level	%
Shandong	26.7%	25.3%	-1.4pp	-5%	18.1%	18.2%	0.0pp	0%	11.4%	12.1%	0.7pp	6%
Shanghai	27.9%	29.7%	1.8pp	7%	19.7%	20.7%	1.0pp	5%	12.3%	11.3%	-1.0pp	-8%
Tianjin	23.5%	25.2%	1.7pp	7%	15.8%	17.8%	1.9pp	12%	9.7%	12.1%	2.3pp	24%
Zhejiang	33.4%	36.0%	2.6pp	8%	22.6%	26.5%	3.9pp	17%	13.6%	15.4%	1.8pp	13%
Panel C: Northeastern region												
Heilongjiang	10.2%	11.2%	1.0pp	9%	6.3%	7.3%	0.9pp	15%	2.9%	4.0%	1.1pp	38%
Jilin	11.1%	12.2%	1.1pp	10%	6.9%	8.5%	1.5pp	22%	3.4%	4.9%	1.5pp	45%
Liaoning	14.4%	15.8%	1.4pp	10%	9.1%	10.3%	1.3pp	14%	5.1%	6.2%	1.1pp	21%
Panel D: Central region												
Anhui	32.7%	32.3%	-0.4pp	-1%	25.2%	23.4%	-1.8pp	-7%	16.2%	15.5%	-0.7pp	-5%
Henan	29.6%	29.4%	-0.2pp	-1%	21.5%	21.1%	-0.4pp	-2%	13.9%	14.5%	0.6pp	4%
Hubei	33.3%	33.9%	0.6pp	2%	25.1%	24.2%	-0.9pp	-3%	16.7%	15.4%	-1.3pp	-8%
Hunan	36.2%	37.6%	1.4pp	4%	25.7%	26.8%	1.1pp	4%	16.5%	17.1%	0.5pp	3%
Jiangxi	38.8%	41.8%	3.0pp	8%	28.1%	31.7%	3.6pp	13%	17.9%	20.9%	3.1pp	17%
Shanxi	16.1%	16.6%	0.5pp	3%	10.6%	11.1%	0.6pp	5%	6.0%	6.6%	0.5pp	9%
Panel E: Western region												
Gansu	11.1%	10.7%	-0.4pp	-3%	6.6%	6.4%	-0.2pp	-3%	3.0%	2.9%	0.0pp	-1%
Guangxi	47.5%	49.2%	1.7pp	4%	33.3%	36.8%	3.4pp	10%	20.2%	21.4%	1.2pp	6%
Guizhou	19.5%	19.4%	-0.1pp	0%	12.2%	11.6%	-0.6pp	-5%	7.0%	6.1%	-0.9pp	-13%
Neimenggu	9.9%	12.0%	2.1pp	21%	6.0%	8.2%	2.2pp	36%	2.9%	4.7%	1.8pp	62%
Ningxia	12.9%	14.1%	1.1pp	9%	8.8%	9.6%	0.8pp	10%	5.0%	5.7%	0.7pp	13%
Qinghai	4.9%	3.8%	-1.1pp	-23%	1.4%	1.0%	-0.4pp	-30%	0.1%	0.0%	-0.1pp	-71%
Shaanxi	19.5%	19.3%	-0.2pp	-1%	13.3%	13.1%	-0.3pp	-2%	8.6%	8.2%	-0.3pp	-4%
Sichuan	28.5%	29.4%	0.8pp	3%	19.3%	19.7%	0.4pp	2%	12.5%	12.2%	-0.3pp	-3%
Xinjiang	16.3%	18.0%	1.6pp	10%	11.4%	13.1%	1.7pp	14%	7.4%	8.8%	1.4pp	18%
Xizang	1.3%	1.4%	0.1pp	5%	0.1%	0.1%	0.0pp	-32%	0.0%	0.0%	0.0pp	159%
Yunnan	19.2%	21.0%	1.8pp	9%	11.0%	12.3%	1.3pp	12%	4.6%	5.3%	0.8pp	17%

Note: We present similar statistics as in Table D.1, but now compute exposures separately for four economic regions and provincial-level administrative units in China. Columns (cols) 4–6 and 7–9 focus on at least moderate UTCI heat exposure at $\geqslant 26\ ^\circ$C and $\geqslant 29\ ^\circ$C, respectively. Cols 1–3 provide UTCI heat exposure at $\geqslant 23\ ^\circ$C, where UTCI 23 °C is a temperature level that is just below the threshold (25 °C) for moderate heat stress. Cols 1 and 2, 5 and 6, and 9 and 10 show the annual average share of time at risk of exposure to heat stress thresholds (UTCI temperatures at $\geqslant z\ ^\circ$C) for children in China (ages 0–14). Cols 3 and 4, 7 and 8, and 11 and 12 show 1990 to 2020 changes in percentage points (level) or percentage (%) of the average shares of time exposed to heat. Cells are empty for percentage changes when the denominator is equal to zero. We consider all 24 hours and 12 months.